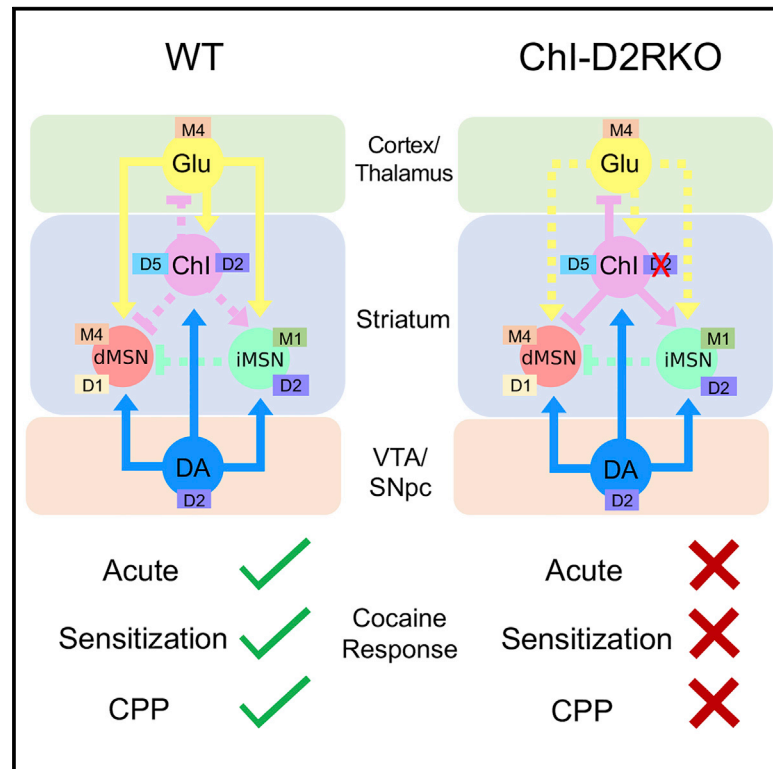**Article**

Dopaminergic Control of Striatal Cholinergic Interneurons Underlies Cocaine-Induced Psychostimulation

Graphical Abstract

Authors

Robert G. Lewis, Marcello Serra,
Daniela Radl, ..., Sharon E. Michalak,
Christopher D. Vanderwal,
Emiliana Borrelli

Correspondence

borrelli@uci.edu

In Brief

Cocaine increases striatal dopamine, which is responsible for the psychomotor effects of the drug. Lewis et al. analyze how alterations of D2R signaling in cholinergic interneurons affect cocaine-mediated responses and show that the absence of D2R reduces the motor response to the drug and abolishes its reinforcing properties.

Highlights

- D2R signaling in ChIs enables the motor and cellular effects of cocaine in male mice

- Absence of D2R in ChIs increases cocaine-dependent striatal ACh signaling

- M4R overactivation in striatal circuits prevents the full response to cocaine

- The reinforcing effects of cocaine are abolished in the absence of D2R in ChIs

CellPress

Article

Dopaminergic Control of Striatal Cholinergic Interneurons Underlies Cocaine-Induced Psychostimulation

Robert G. Lewis,[1] Marcello Serra,[1] Daniela Radl,[1] Michela Gori,[1] Catherine Tran,[1] Sharon E. Michalak,[2] Christopher D. Vanderwal,[2] and Emiliana Borrelli[1,3,*]

[1]Department of Microbiology & Molecular Genetics, U1233 INSERM, Center for Epigenetics and Metabolism, University of California, Irvine, Irvine, CA 92697, USA
[2]Department of Chemistry, University of California, Irvine, Irvine, CA 92697, USA
[3]Lead Contact
*Correspondence: borrelli@uci.edu
https://doi.org/10.1016/j.celrep.2020.107527

SUMMARY

Cocaine drastically elevates dopamine (DA) levels in the striatum, a brain region that is critical to the psychomotor and rewarding properties of the drug. DA signaling regulates intrastriatal circuits connecting medium spiny neurons (MSNs) with afferent fibers and interneurons. While the cocaine-mediated increase in DA signaling on MSNs is well documented, that on cholinergic interneurons (ChIs) has been more difficult to assess. Using combined pharmacological, chemogenetic, and cell-specific ablation approaches, we reveal that the D2R-dependent inhibition of acetylcholine (ACh) signaling is fundamental to cocaine-induced changes in behavior and the striatal genomic response. We show that the D2R-dependent control of striatal ChIs enables the motor, sensitized, and reinforcing properties of cocaine. This study highlights the importance of the DA- and D2R-mediated inhibitory control of ChIs activity in the normal functioning of striatal networks.

INTRODUCTION

Cocaine elevates dopamine (DA) levels in the brain by blocking the DA transporter (Cone, 1995; Hyman et al., 2006). This leads to increased DA signaling in areas receiving dopaminergic afferents, including the striatum. The striatum is subdivided in functional districts, with the dorsal area involved in the control of movement and action selection (Graybiel et al., 1994; Marche et al., 2017; Surmeier et al., 2009) and the ventral area mostly implicated in reward processing (Carelli, 2002; Day et al., 2007). The medium spiny neurons (MSNs) are the major constituent of the striatum, representing 90%–95% of the neuronal population, while a minor population is made up of interneurons (5%–10%) (Graveland and DiFiglia, 1985; Oorschot, 2013). MSNs are GABAergic neurons that project either directly (dMSNs) or indirectly (iMSNs) to output structures of the basal ganglia (Nelson and Kreitzer, 2014). The expression of stimulatory DA D1 receptors (D1Rs) defines dMSNs, while iMSNs are characterized by the

expression of inhibitory DA D2 receptors (D2Rs). Thus, the elevation of DA levels that follows cocaine intake activates dMSNs and inhibits iMSNs (Lobo and Nestler, 2011).

Striatal cholinergic interneurons (ChIs) represent 1%–2% of the striatal cell population; DA signaling is simultaneously inhibitory through D2R (Kharkwal et al., 2016a; Oldenburg and Ding, 2011; Pisani et al., 2000) and excitatory through D5R (Berlanga et al., 2005; Centonze et al., 2003) on ChIs activity and ACh release (DeBoer and Abercrombie, 1996). At the same time, ACh inhibits dMSNs through activation of muscarinic type 4 receptors (M4R) (Jeon et al., 2010; Mamaligas and Ford, 2016; Threlfell et al., 2010) and excites iMSNs through M1Rs (Moehle et al., 2017; Shen et al., 2007). Thus, due to the reciprocal functional control of MSNs and ChIs, altering the striatal DA-ACh balance (Aosaki et al., 2010) has major consequences for MSNs, which are the sole output of the striatum.

At the level of intracellular signaling, the cocaine-dependent increase in DA activates cAMP and ERK pathways in dMSNs which leads to the increased expression of immediate early genes, such as *c-fos* and other signaling molecules (Hyman and Malenka, 2001; Philibin et al., 2011; Valjent et al., 2000). These effects are mediated by the activation of D1R, since they are absent upon the administration of D1R antagonists or in D1R-knockout (KO) mice (Xu et al., 1994; Young et al., 1991). Nevertheless, the dMSNs-mediated motor response to cocaine and the induction of *c-fos* in these same neurons require intact D2R signaling in iMSNs (Kharkwal et al., 2016b; Lemos et al., 2016). It has been proposed that this effect depends on increased GABAergic signaling within striatal circuits in the absence of D2R in iMSNs (Centonze et al., 2004; Kharkwal et al., 2016b; Lemos et al., 2016).

Due to their low abundance, the influence of ChIs on the overall regulation of striatal circuitries has been difficult to assess. Furthermore, D2R-mediated modulation of ChIs in the context of cocaine response has not been fully explored *in vivo*. In this study, we sought to address this gap in knowledge by analyzing the response to cocaine of ChI-D2RKO mice lacking inhibitory D2R signaling in ChIs. These mice are characterized by normal motor behavior in basal conditions (Kharkwal et al., 2016a). Here, we explored the motor, sensitizing, and reinforcing properties of cocaine in ChI-D2RKO mice in comparison to wild-type (WT) littermates.
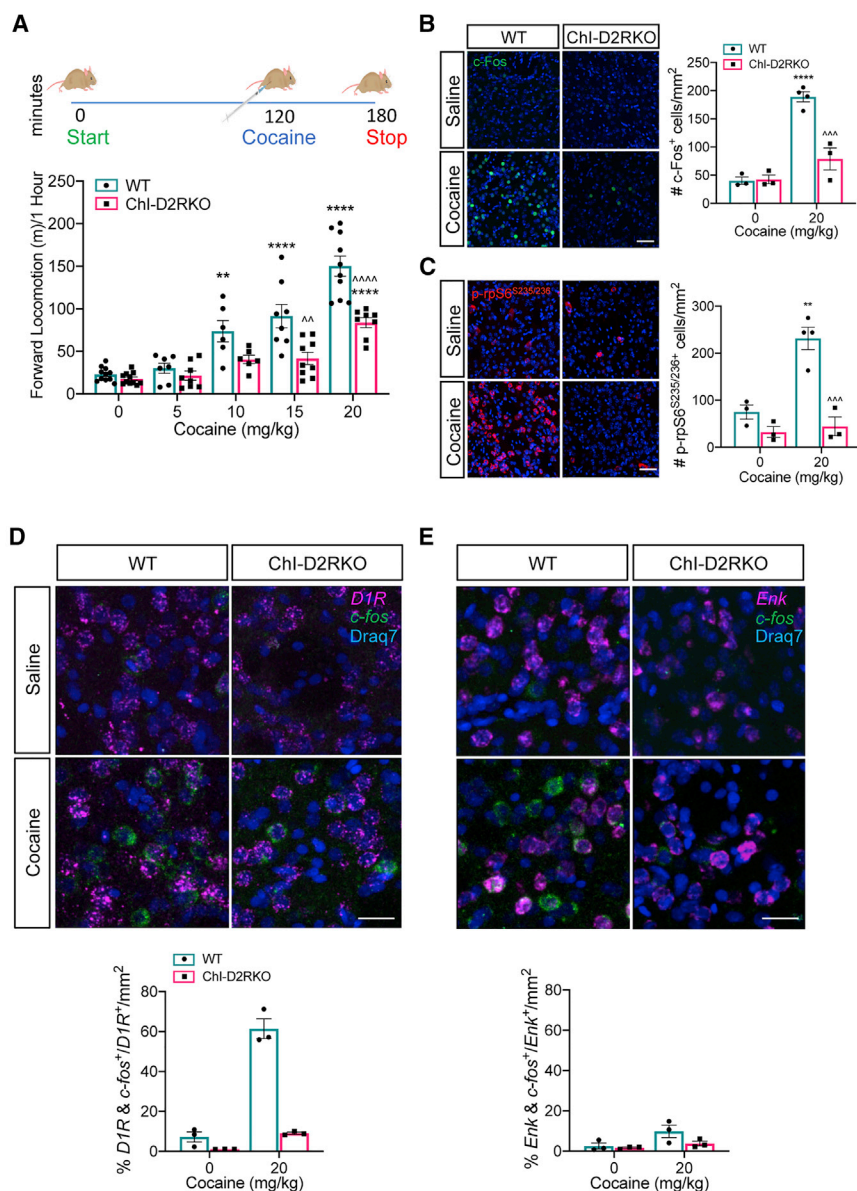
Figure 1. Absence of D2R Signaling in ChIs Leads to Reduced Cocaine Response

(A) Top: protocol followed for studying cocaine effects. Bottom: cocaine dose-dependent induction of motor activity in WT and ChI-D2RKO mice (n = 6–11/group). Genotype: $F_{(1, 4)}$ = 41.54, p < 0.0001; treatment: $F_{(4, 74)}$ = 53.19, p < 0.0001; interaction: $F_{(4, 74)}$ = 6.121, p = 0.0003.

(B and C) Left: representative images of IF experiments in cocaine-treated WT and ChI-D2RKO mice using (B) c-Fos and (C) p-rpS6$^{S235/236}$ antibodies. Right: (B) quantifications of c-Fos$^+$ neurons (genotype: $F_{(1, 9)}$ = 21.92, p = 0.0009; treatment: $F_{(1, 9)}$ = 63.97, p < 0.0001; interaction: $F_{(1, 9)}$ = 23.85, p = 0.0011) in (C) quantifications of p-rpS6$^{S235/236+}$ neurons (genotype: $F_{(1, 9)}$ = 33.12, p = 0.0003; treatment: $F_{(1, 9)}$ = 17.90, p = 0.0022; interaction: $F_{(1, 9)}$ = 13.17, p = 0.0055) (n = 3–4/group).

(D and E) Top: representative images of FISH experiments using (D) *D1R* or (E) *Enk* riboprobes along with *c-fos* riboprobes, as indicated. Bottom: percentage of double positive cells over the total number of (left) *D1R$^+$* or (right) *Enk$^+$* neurons per square millimeter.

**p < 0.01, **p < 0.001 ****p < 0.0001 versus saline of same genotype; ^^p < 0.01, ^^^^p < 0.0001 versus WT with same treatment. Scale bars for (B) and (C): 50 μm; for (D) and (E): 25 μm. In (A)–(E), bars represent the means ± SEMs.

tion. We propose that D2R signaling exerts major control over ChIs and ACh release, which is required for the normal functioning of striatal circuits.

RESULTS

Absence of D2R Signaling in ChIs Leads to Reduced Cocaine Response

We previously generated ChI-D2RKO mice carrying the selective ablation of D2R in ChIs and showed that under basal conditions, motor activity is intact in these mice (p = 0.1247) (Figure S1A) (Kharkwal et al., 2016a). In this study, we analyzed the motor and reinforcing properties of cocaine in ChI-D2RKO mice. We hypothesized that cocaine-induced DA elevation would generate a stronger response of ChIs in the absence of D2R in ChI-D2RKO mice as compared to WT siblings. Stimulation of D1-like receptors on ChIs in the absence of the inhibitory D2R signaling may lead to increased ACh signaling in the striatum.

A cocaine dose-response curve was made to compare the motor response of male ChI-D2RKO mice to their WT littermates. Cocaine (5, 10, 15, and 20 mg/kg) or saline was injected intraperitoneally (i.p.) and motor activity recorded for 1 h in a novel home cage (NHC). While WT mice dose dependently respond to cocaine with an increase in their horizontal locomotion, the response of ChI-D2RKO mice was significantly attenuated

Notably, we found that the acute and sensitized motor response to cocaine was severely lowered in ChI-D2RKO mice. The behavioral phenotype was paralleled by the loss of induction of *c-fos* and other striatal genes that are typically elevated by cocaine (Gao et al., 2017; Hope et al., 2006; McClung and Nestler, 2003; Thiriet et al., 2000). These effects are assigned to increased ACh signaling in ChI-D2RKO mice, as shown by the reversal of the behavioral and cellular phenotypes in these mice by chemogenetic silencing of ChIs or by blocking muscarinic M4R signaling. We found that not only is the motor response affected in ChI-D2RKO mice but also the reinforcing properties of cocaine were reduced.

Our study emphasizes the importance of the dopaminergic control on cholinergic tone in striatal responses to cocaine and may pave the way for future therapeutic strategies to treat addic-

(p = 0.0003) (Figure 1A). Although WT mice show a significant motor response to cocaine starting at 10 mg/kg compared to saline-treated mice of the same genotype (p = 0.0016), ChI-D2RKO mice displayed a significant response to the drug only at 20 mg/kg (p < 0.0001), the highest dose tested, which was nonetheless ~40% lower than that of equally treated WT mice (p < 0.0001).

The cocaine-driven increase in DA and glutamate signaling in dMSNs is reflected in the induction of the immediate early gene c-Fos in the dorsomedial striatum (DMS) and the ventral striatum (Jenab et al., 2003; Torres and Rivier, 1993) and of post-translational modifications involving the phosphorylation of the ribosomal protein S6 on the serine residues 235/236 (p-rpS6$^{S235/236}$) (Puighermanal et al., 2017). p-rpS6$^{S235/236}$ requires only DA D1R-mediated activation of the cAMP pathway in dMSNs, which is different from that of c-fos induction (Biever et al., 2015). Therefore, analyzing levels of c-fos and rpS6$^{S235/236}$ phosphorylation served as monitors of dopaminergic and cortical inputs to dMSNs. Thus, striatal brain sections from WT and ChI-D2RKO mice were analyzed 1 h after saline or cocaine by immunofluorescence (IF) using antibodies directed against c-Fos and p-rpS6$^{S235/236}$. We observed a significantly reduced number of c-Fos^{+} cells in the DMS of ChI-D2RKO mice as compared to equally treated WT controls (p = 0.0004) (Figure 1B). The same decrease was observed in the ChI-D2RKO ventral striatum (p < 0.0001) (Figure S1B). In parallel, a lower number of p-rpS6$^{S235/236+}$ cells were observed in the DMS (p = 0.0004) (Figure 1C) and the ventral striatum (p = 0.0118) of ChI-D2RKO mice in comparison to WT mice (Figure S1C). The reduced induction of c-Fos affected dMSNs, as shown by double fluorescent in situ hybridization (FISH) on the striatal tissue sections, hybridized with a c-fos-specific riboprobe along with either a D1R-specific probe as a marker of dMSNs or an enkephalin (Enk) probe to label iMSNs. Quantifications of FISH analyses showed that in cocaine-treated WT striata, c-fos induction was observed in 61% of D1R^{+} dMSNs (Figure 1D) and only 9% in Enk^{+} iMSNs (Figure 1E). In contrast, c-fos^{+} neurons were estimated at 9% in D1R^{+} dMSNs and 4% of Enk^{+} iMSNs in cocaine-treated ChI-D2RKO mice. These results show that D2R expression in ChIs is required for the well-known behavioral and cellular effects of cocaine in dMSNs.

Altered Transcriptomic Profile in the Striatum of ChI-D2RKO Mice

Loss of c-Fos induction in response to cocaine in ChI-D2RKO striata prompted us to perform an unbiased analysis to identify the genes that were differentially expressed in the DMS between WT and ChI-D2RKO using RNA sequencing (RNA-seq). Male WT and ChI-D2RKO mice (n = 4/group) were administered a single injection of saline or cocaine (20 mg/kg, i.p.) and sacrificed 1 h later. RNAs from the DMS were then prepared and processed for RNA-seq.

Saline-treated WT and ChI-D2RKO striata had a total of 871 differentially expressed transcripts, 365 were downregulated and 506 were upregulated in WT mice as compared to ChI-D2RKO mice (Figure S2A). After cocaine, differential expression analyses revealed a total of 969 differentially expressed transcripts between the 2 genotypes (p < 0.05) (Figure S2B). This is composed of 595 transcripts upregulated and 374 downregu-

lated by cocaine; only 59 genes were found to be in common in these 2 analyses (Figure S2C). Among all differentially expressed transcripts identified in cocaine-treated mice, we extracted 60 highly significant genes (padj < 0.05), which represent the bona fide signature of cocaine-induced genomic response (Figure 2A) (Chandra and Lobo, 2017; Fosnaugh et al., 1995; Gonzales et al., 2019; Hope et al., 1992; McClung and Nestler, 2003).

Consistent with our previous IF analyses, c-fos was found among the most significant differentially expressed genes (p = 7.91 * 10^{-22}) (Figures 2A and 2B). In addition to c-fos, other members of the AP-1 transcription factor complex—Fosb, Fosl2, and Junb (Curran and Franza, 1988; Su et al., 2017)—and of the nuclear receptor subfamily 4 group A—Nr4a1 and Nr4a3 (Volakakis et al., 2010)—together with early growth response transcription factors Egr1, Egr2, Egr3, and Egr4 (Duclot and Kabbaj, 2017; Gao et al., 2017), were induced in the WT, but not in the ChI-D2RKO DMS (Figures 2A and 2B).

Gene Ontology analyses performed using the Database for Annotation, Visualization, and Integrated Discovery (DAVID) indicated that differentially expressed genes with significant fold changes found in cocaine-treated mice (Figure 2B, red), were heavily involved in the regulation of transcription. Functional annotation categories such as "positive regulation of transcription," "transcription from RNA pol II promoter," and "transcription factor binding" were highly significant (Figure 2C).

Thus, we performed an enrichment analysis using ChEA3 (Keenan et al., 2019) to identify transcription factors that putatively regulate the 969 differentially expressed genes in cocaine-treated mice (Figure S2B). Of the top 25 transcription factors enriched for targeting our gene set, 10 were found among our most significant differentially expressed genes (Figures 2A and 2D). Each of the 10 transcription factors identified was increased in WT but not in ChI-D2RKO mice (Figures 2A and 2D). Thus, the loss of induction of genes previously identified as genomic signatures of the effects of cocaine indicates that the inhibitory dopaminergic control exerted by D2R on ACh signaling enables the acute induction of gene expression.

Elevated ChI Activity Mediates Deficits in the ChI-D2RKO Mouse Response to Cocaine

We hypothesized that the lowered response to cocaine of ChI-D2RKO mice originates from increased ACh signaling in the striatum generated by the absence of the modulatory D2R in ChIs. To validate our hypothesis, we treated male WT mice with the acetylcholinesterase inhibitor donepezil, which blocks ACh degradation (Karvat and Kimchi, 2014). We administered saline or donepezil (1 mg/kg, i.p.) 15 min before cocaine and evaluated motor activity for the following hour. In line with our hypothesis, donepezil administration before cocaine severely abates the motor response of WT mice as compared to cocaine only treated animals (p < 0.0001) (Figure 3A).

Next we sought to directly show that increased ACh signaling in the DMS is responsible for the reduced response to cocaine of ChI-D2RKO. We used a chemogenetic approach to specifically silence ChI activity in ChI-D2RKO mice using the designer receptor exclusively activated by designer drugs (DREADD), hM4Di, upon the administration of clozapine-N-oxide (CNO) or JHU37160 (J60). For this purpose, we performed stereotaxic
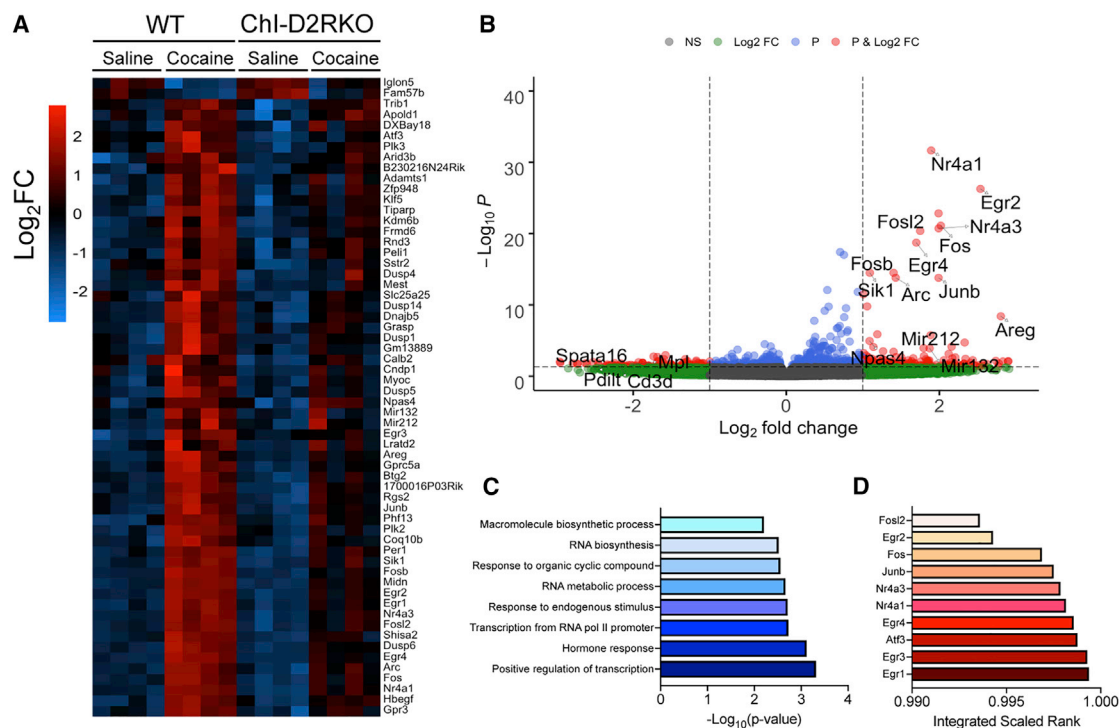
Figure 2. Altered Transcriptomic Profile in the Striatum of ChI-D2RKO Mice

(A) Heatmap illustrating the log2-fold change (log$_2$FC) of genes differentially expressed (padj < 0.05) in cocaine-treated (20 mg/kg, i.p.) WT and ChI-D2RKO mice; upregulation (red) downregulation (blue).

(B) Volcano plot based on the −log10 p value (−log$_{10}$P) versus the log$_2$FC of the DMS transcriptome. Cutoffs are shown as dotted lines (p < 0.05) and log$_2$FC ± 1.

(C) Gene Ontology determined by DAVID using genes with p < 0.05 and log$_2$FC above 1 and below −1 (shown in red in (B).

(D) Transcription factor enrichment analysis of the 969 differentially expressed genes (see Figure S2B) using ChEA3. The top 25 enriched transcription factors were compared with the most significant genes (padj < 0.05); the resulting integrated scaled rank of 10 transcription factors is shown.

injections of the adeno-associated viral vector carrying hM4Di (Roth, 2016), whose expression is Cre-recombinase dependent, into the DMS of ChI-D2RKO mice. Two weeks after surgery, we analyzed and confirmed the specific expression of hM4Di in ChIs by IF using antibodies directed against the mCherry tag of hM4Di along with choline acetyltransferase (ChAT), a ChI marker (Figure S3A). We confirmed that CNO (3 mg/kg, i.p.) and J60 (0.1 mg/kg, i.p.) (Bonaventura et al., 2018) did not affect locomotion in the absence of cocaine in hM4Di expressing ChI-D2RKO mice (hM4Di ChI-D2RKO) throughout 7 days of exposure (p = 0.7071) (Figure S3B).

Next, hM4Di ChI-D2RKO were treated with CNO (3 mg/kg, i.p.) 30 min before cocaine (15 mg/kg, i.p.) and motor activity recorded for the following hour. hM4Di ChI-D2RKO showed a response to cocaine upon CNO administration that was significantly increased from that of ChI-D2RKO mice not expressing hM4Di (p < 0.0002) or to saline-treated hM4Di ChI-D2RKO mice (p = 0.0002). The hM4Di ChI-D2RKO mice response to cocaine did not differ from that of WT mice (p > 0.99) (Figure 3B).

Cocaine Sensitization in Mice with a Deletion of D2R in ChIs

Repeated intake of cocaine causes maladaptive changes in the mesolimbic dopamine system that lead to an enhanced motor response to the drug (Boudreau and Wolf, 2005; Kalivas and Stewart, 1991; Robinson and Berridge, 2008). Thus, we focused on determining whether the behavioral deficits of ChI-D2RKO mice observed after acute administration would also affect cocaine sensitization. To test this, male mice that were habituated to a home cage for 2 days were then administered cocaine (15 mg/kg, i.p.) daily for 5 days and had their motor activity recorded for 1 h. Chronic cocaine administration induced a linear increase in the motor activity in all of the mice tested (Figure 3C). ChI-D2RKO mice also showed a significant increase in the motor response between days 1 and 5 (p = 0.0204); however, their response was significantly lower than that of cocaine-treated WT mice (p = 0.0001) (Figures 3C and 3D). We then assessed whether silencing ChIs using the DREADD system in the DMS may restore cocaine sensitization to WT levels. In line with previous results, hM4Di ChI-D2RKO mice treated with CNO (3 mg/kg, i.p.) before cocaine, during the 5 days of repeated administration, increased motor activity as compared to ChI-D2RKO mice not expressing hM4Di (p < 0.0001) (Figure 3C). The response of hM4Di ChI-D2RKO mice treated with cocaine and CNO did not differ from that of WT mice treated with cocaine. Similar results were obtained using J60 (0.1 mg/kg, i.p.) (p < 0.0001) (Figure S3C), thereby excluding the possible interference of CNO with DA receptors.
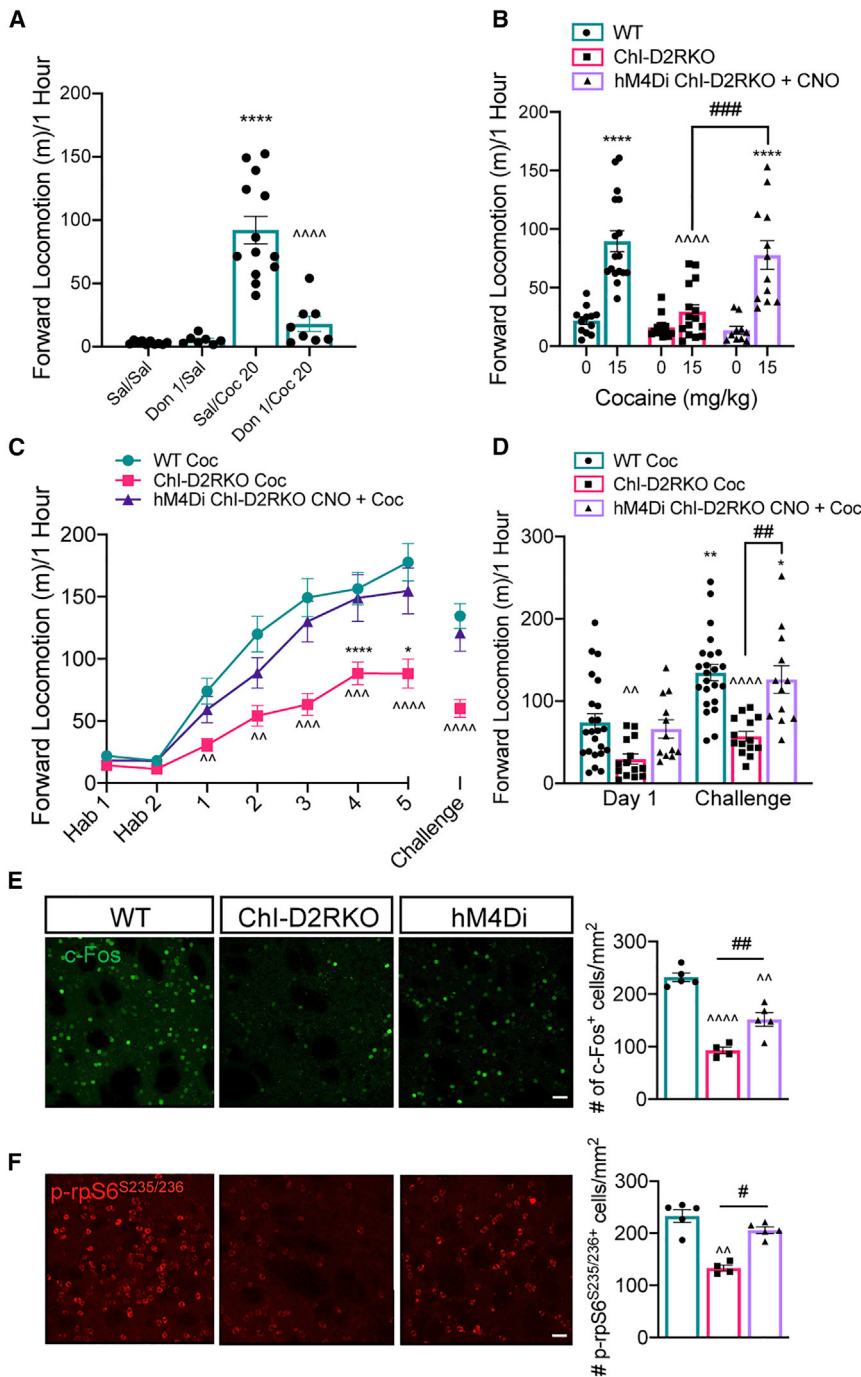
Figure 3. Cocaine Sensitization in Mice with a Deletion of D2R in ChIs

(A) Donepezil lowers the motor response to cocaine in WT mice (n = 7–13/group). Treatment: $F_{(3, 34)} = 33.30$, $p < 0.0001$. Bonferroni test: ****$p < 0.0001$ versus Sal/Sal; ^^^^$p < 0.0001$ versus Sal/Coc 20.

(B) Silencing of ChIs in ChI-D2RKO mice restores acute cocaine response (n = 10–14/group). Genotype: $F_{(1, 9)} = 33.12$, $p = 0.0003$; treatment: $F_{(1, 9)} = 17.90$, $p = 0.0022$; interaction: $F_{(1, 9)} = 13.17$, $p = 0.0055$. Bonferroni test: ****$p < 0.0001$ versus saline in the same genotype; ^^^^$p < 0.0001$ versus WT Coc; ###$p < 0.001$ versus ChI-D2RKO Coc.

(C) Locomotor sensitization to cocaine (n = 14–22/group). Genotype: $F_{(2, 48)} = 12.57$, $p < 0.0001$; day: $F_{(7, 336)} = 82.06$, $p < 0.0001$; interaction: $F_{(14, 336)} = 3.633$, $p < 0.0001$. Bonferroni test: *$p < 0.05$, ****$p < 0.0001$, versus day 1 in mice of the same genotype; ^^$p < 0.01$, ^^^$p < 0.001$, ^^^^$p < 0.0001$ versus WT on the same day.

(D) Comparison of motor responses on day 1 and the challenge day from (C). Genotype: $F_{(2, 48)} = 12.57$, $p < 0.0001$; day: $F_{(7, 336)} = 82.06$, $p < 0.0001$; interaction: $F_{(14, 336)} = 3.633$, $p < 0.0001$. Bonferroni test: *$p < 0.05$, **$p < 0.01$, versus day 1 in mice with the same genotype; ^^$p < 0.01$, ^^^^$p < 0.0001$ versus WT on the same day of the experiment; ##$p < 0.01$ versus ChI-D2RKO on the same day.

(E and F) Left: representative images of IF experiments. Right: (E) quantification per square millimeter of c-Fos+ neurons (genotype: $F_{(2, 12)} = 35.28$, $p < 0.0001$) and (F) quantifications per square millimeter of p-rpS6$^{S235/236+}$ neurons (genotype: $F_{(2, 16)} = 9.686$; $p = 0.0018$) of IF experiments in the DMS 1 h after the challenge (n = 4/group). Bonferroni test: ^^$p < 0.01$, ^^^^$p < 0.0001$ versus WT; #$p < 0.05$, ##$p < 0.01$ versus ChI-D2RKO.

Values in (A)–(F) are means ± SEMs. Scale bars: 50 μm.

To further verify the long-term effect of sensitization in mice of both genotypes, we left mice untreated for 7 days and then challenged them with a lower dose of cocaine (10 mg/kg, i.p.). While WT mice showed a sensitized response after the withdrawal period, ChI-D2RKO mice did not. The response to the cocaine challenge of ChI-D2RKO mice did not differ from the one observed on the first day of cocaine treatment (p > 0.99) (Figure 3D). Consistent with elevated ACh levels being responsible for the impaired sensitization of ChI-D2RKO mice, hM4Di ChI-

D2RKO mice treated with CNO showed cocaine sensitization that did not differ from that of WT mice (p > 0.99) (Figure 3C). Interestingly, induction of both c-Fos expression (Figure 3E) and rpS6$^{S235/236}$ phosphorylation (Figure 3F) 1 h after the challenge injection were increased in hM4Di ChI-D2RKO mice given CNO and cocaine (c-Fos: p = 0.0057; p-rpS6$^{S235/236}$: p = 0.0006) as compared to ChI-D2RKO mice not expressing hM4Di. Similar results were obtained using J60 and cocaine in hM4Di ChI-D2RKO mice (p = 0.0310) (Figure S3D).

Antagonism of Muscarinic Receptors Enables Cocaine Response in ChI-D2RKO Mice

ACh in the striatum activates muscarinic and nicotinic receptors (Lim et al., 2014). MSNs are major targets of ACh signaling dependent on the activation of muscarinic M4R and M1R. To elucidate the mechanism underlying the weakened response of
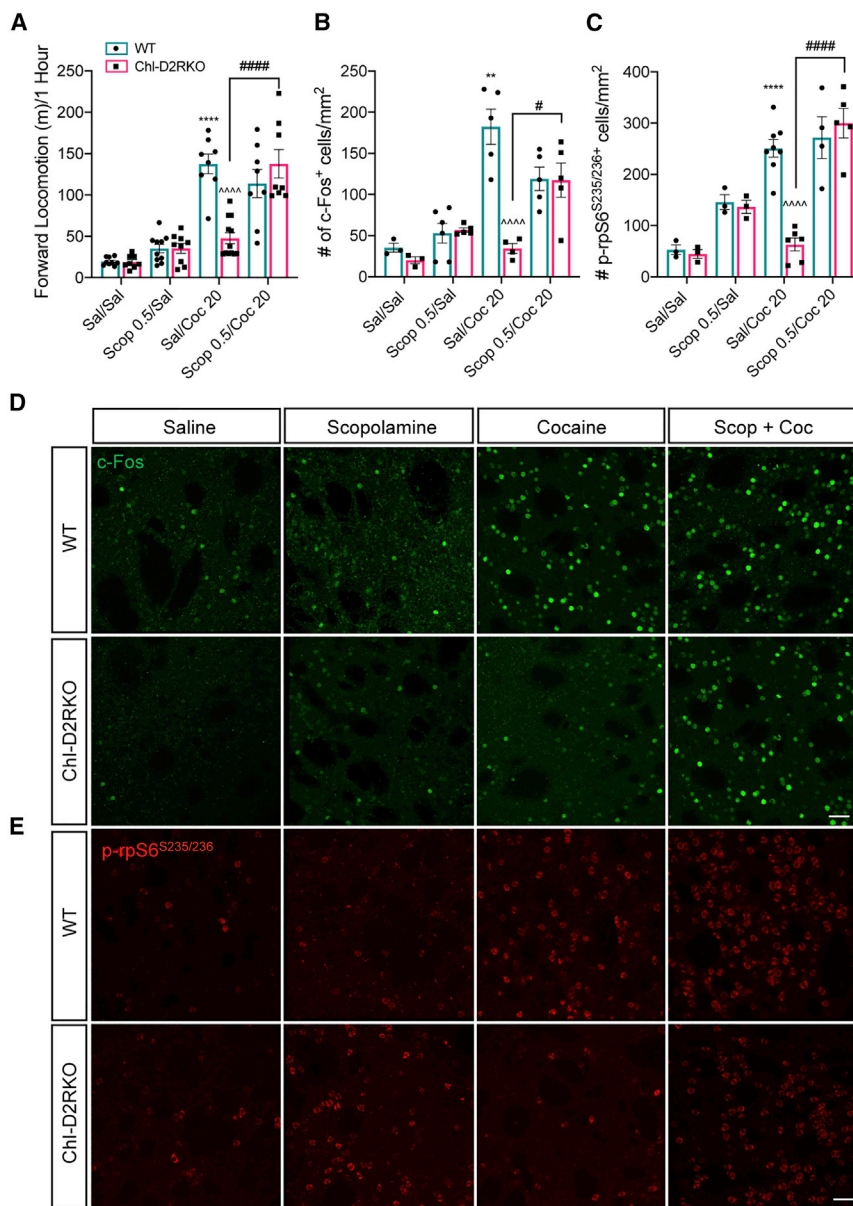
Figure 4. Antagonism of Muscarinic Receptors Enables Cocaine Response in Chl-D2RKO Mice

(A) Motor activity in the presence or absence of scopolamine administered 15 min before cocaine (n = 8–12/group). Genotype: $F_{(1, 64)}$ = 5.971, p = 0.0173; treatment: $F_{(3, 64)}$ = 51.346, p < 0.0001; interaction: $F_{(3, 64)}$ = 14.22, p < 0.0001.

(B and C) (B) Quantification of the number of c-Fos^{+} positive neurons (genotype: $F_{(1, 28)}$ = 14.19, p = 0.0008; treatment: $F_{(3, 28)}$ = 15.47, p < 0.0001; interaction $F_{(3, 28)}$ = 12.26, p < 0.0001) and (C) quantification of p-rpS6$^{S235/236+}$ positive neurons (genotype: $F_{(1, 27)}$ = 11.79, p < 0.0001; treatment: $F_{(3, 27)}$ = 31.41, p < 0.0001; interaction $F_{(3, 27)}$ = 6.640, p = 0.0158) neurons per square millimeter within the DMS 1 h after cocaine (n = 3–6/group). For (A)–(C), Bonferroni test: *p < 0.05, **p < 0.01, ****p < 0.0001 versus saline of same genotype; ^^^^p < 0.0001 versus WT Coc 20; #p < 0.05, ##p < 0.01, ###p > 0.001, ####p < 0.0001 versus treatment within the same genotype. All of the values are means ± SEMs.

(D and E) (D) Representative images of c-Fos^{+} neurons and (E) representative images of p-rpS6$^{S235/236+}$ neurons in the DMS of mice treated as in (A)–(C). Scale bars: 50 μm.

(Figure 4A). For each genotype, male mice were divided into 4 groups: saline, scopolamine (0.5 mg/kg, i.p.), cocaine (20 mg/kg, i.p.), or the combination of both. Scopolamine was administered 15 min before saline or cocaine and forward locomotion recorded for 1 h after the last injection. The combination of scopolamine and cocaine specifically increased the motor response of Chl-D2RKO mice to cocaine as compared to cocaine-only-treated mice of the same genotype (p < 0.0001) (Figure 4A); this increase resulted in the absence of differences in forward locomotion between Chl-D2RKO and WT mice (p > 0.99).

Chl-D2RKO mice to cocaine, we sought to determine whether muscarinic signaling was involved. Accordingly, we tested the effect on motor activity of the non-selective muscarinic antagonist scopolamine before cocaine administration. To perform these experiments, we controlled that Chl-D2RKO mice could respond to scopolamine as WT mice with an increase in their forward locomotion by performing a dose-response experiment using 0.5 and 1.0 mg/kg scopolamine. At 0.5 mg/kg scopolamine, mice of both genotypes showed a trend toward an increase in motor activity that did not reach statistical significance (p > 0.99), while at the dose of 1 mg/kg, both WT and Chl-D2RKO mice showed a significant increase in motor activity (p < 0.0001) of similar intensity as compared to saline-treated mice of both genotypes (Figure S4). The sub-threshold dose of 0.5 mg/kg was then chosen to perform experiments with cocaine

Blocking muscarinic signaling also translated into the cellular rescue of c-Fos induction and of rpS6 phosphorylation, as assessed by IF quantifications of the number of neurons that were positive for c-Fos (p = 0.0128) (Figures 4B and 4D) and for p-rpS6$^{S235/236}$ (p < 0.0001) (Figures 4C and 4E) in the DMS of Chl-D2RKO and WT mice analyzed 1 h after cocaine administration. These results indicate that the elevated muscarinic signaling is responsible for the reduced motor and cellular responses to cocaine in Chl-D2RKO mice.

The Inhibitory Control of D2R on ChIs Prevents M4R Over-activation

Next, we analyzed whether the behavioral and cellular phenotypes of Chl-D2RKO mice may depend on the increased ACh stimulation of M4R and/or M1R. While M4R activation could
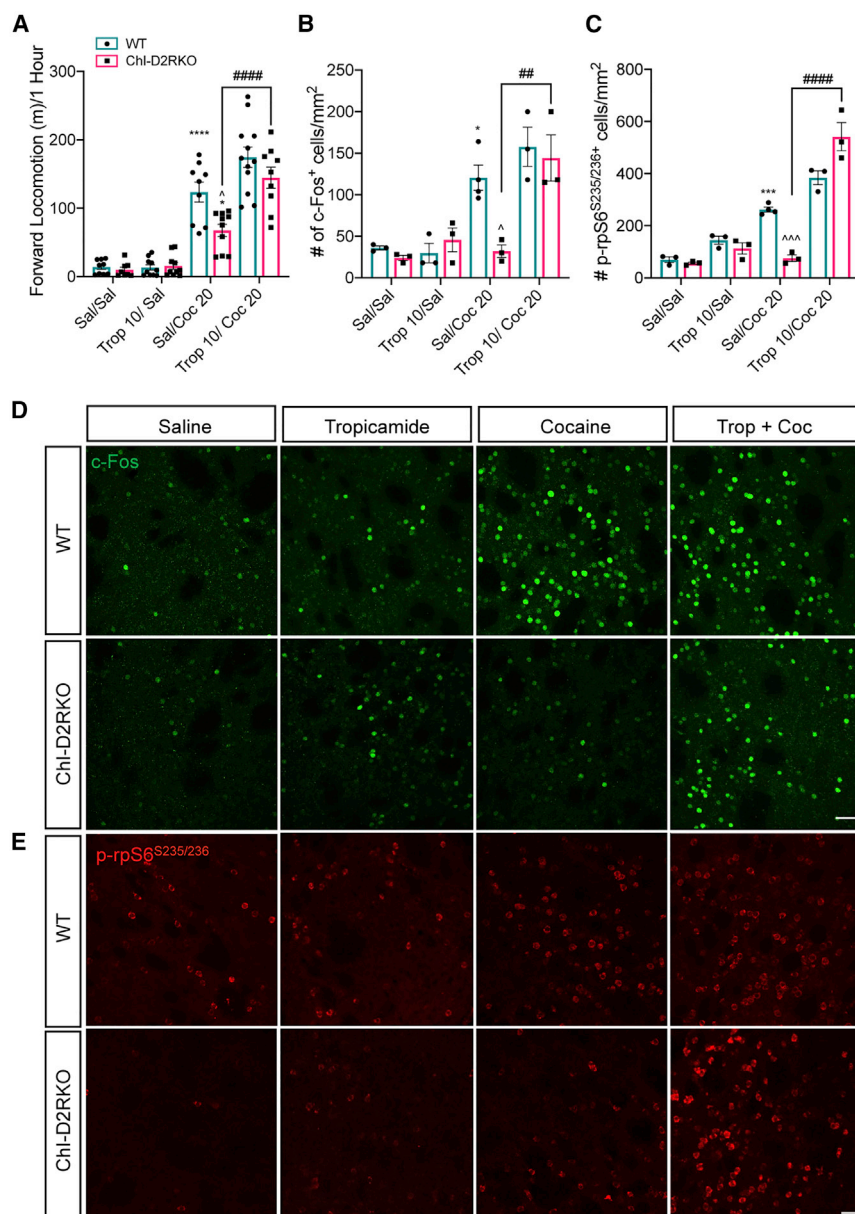
Figure 5. Antagonism of Muscarinic Receptors Enables Cocaine Response in ChI-D2RKO Mice

(A) Tropicamide given 15 min before cocaine restores the cocaine effects in ChI-D2RKO mice (n = 8–11/group). Genotype: $F_{(1, 69)}$ = 8.413, p < 0.0050; treatment: $F_{(3, 69)}$ = 90.63, p < 0.0001; interaction: $F_{(3, 69)}$ = 3.126, p = 0.0313.

(B and C) Quantification of the number of c-Fos$^+$ neurons (genotype: $F_{(1,17)}$ = 4.744, p = 0.0438; treatment: $F_{(3,17)}$ = 23.53, p < 0.0001; interaction: $F_{(3,17)}$ = 4.213, p = 0.0212) (B) and of p-rpS6$^{S235/236+}$ (C) neurons per square millimeter within the DMS 1 h after cocaine (N = 3–6/group) (genotype: $F_{(1, 17)}$ = 1.230, p = 0.2828; treatment: $F_{(3, 17)}$ = 110.3, p < 0.0001; interaction: $F_{(3, 17)}$ = 18.60, p < 0.0001).

Bonferroni test: *p < 0.05, ***p < 0.001, ****p < 0.0001 versus saline of same genotype; ^p < 0.05, ^^^p < 0.001 versus WT Sal/Coc 20; #p < 0.05, ##p < 0.01, ####p < 0.0001 versus ChI-D2RKO Sal/Coc 20.

(D and E) Representative images of (D) c-Fos$^+$ neurons and (E) p-rpS6$^{S235/236+}$ neurons in the DMS of mice treated as in (A)–(C). Scale bars: 50 μm.

Values shown in (A)–(C) are means ± SEMs.

directly inhibit dMSNs, M1R activation of iMSNs could indirectly lead to the inhibition of dMSNs through GABAergic collaterals of iMSNs (Kharkwal et al., 2016b; Lemos et al., 2016).

Thus, male ChI-D2RKO and WT littermates were administered either M4R- or M1R-selective antagonists 15 min before cocaine. Mice of each genotype received either saline, the M4R-selective antagonist, tropicamide (10 mg/kg, i.p.), or the M1R-selective antagonist VU0255035 (60 mg/kg, i.p.) (Sheffler et al., 2009) in the presence or absence of cocaine (20 mg/kg, i.p.). Forward locomotion was recorded for 1 h following cocaine administration. Our results show that the selective blockade of M4R before cocaine rescues the motor-inducing effects of cocaine in the ChI-D2RKO mice to WT levels as compared to the cocaine-only group of the same genotype (p < 0.0001) (Figure 5A). Mirroring the effect

of tropicamide on motor activity, the number of c-Fos$^+$ (p = 0.0036) and p-rpS6$^{S235/236+}$ (p < 0.0001) neurons was significantly increased in ChI-D2RKO mice when this antagonist was administered before cocaine as compared to cocaine-only-treated mice (Figures 5B–5E). Overall, the presence of tropicamide abolished the observed differences between cocaine-treated WT and ChI-D2RKO mice (p > 0.99).

In contrast, blockade of M1R with VU0255035 had a negative effect as it reduced cocaine response in WT mice as compared to the cocaine-only group (p = 0.0003), while it had no effect on the motor activity of cocaine-treated ChI-D2RKO mice with or without VU0255035 (p = 0.2599) (Figure 6A). At the intracellular level, M1R antagonism significantly lowered cocaine-mediated c-Fos induction in WT mice (p = 0.0002) (Figures 6B and 6D). However, the only positive effect of VU0255035 pretreatment on ChI-D2RKO was a significant increase in the number of p-rpS6$^{S235/236+}$ neurons (p = 0.0025) (Figures 6C and 6E). This increase may be caused by a direct effect of the M1R antagonist on dMSNs or alternative undefined mechanisms of M1R antagonism in the striatum.

The Reinforcing Properties of Cocaine Are Affected by the Loss of Dopaminergic Inhibition of ChIs

Next, we aimed at studying the effect of the loss of the dopaminergic inhibition on ChIs on reward-related mechanisms by
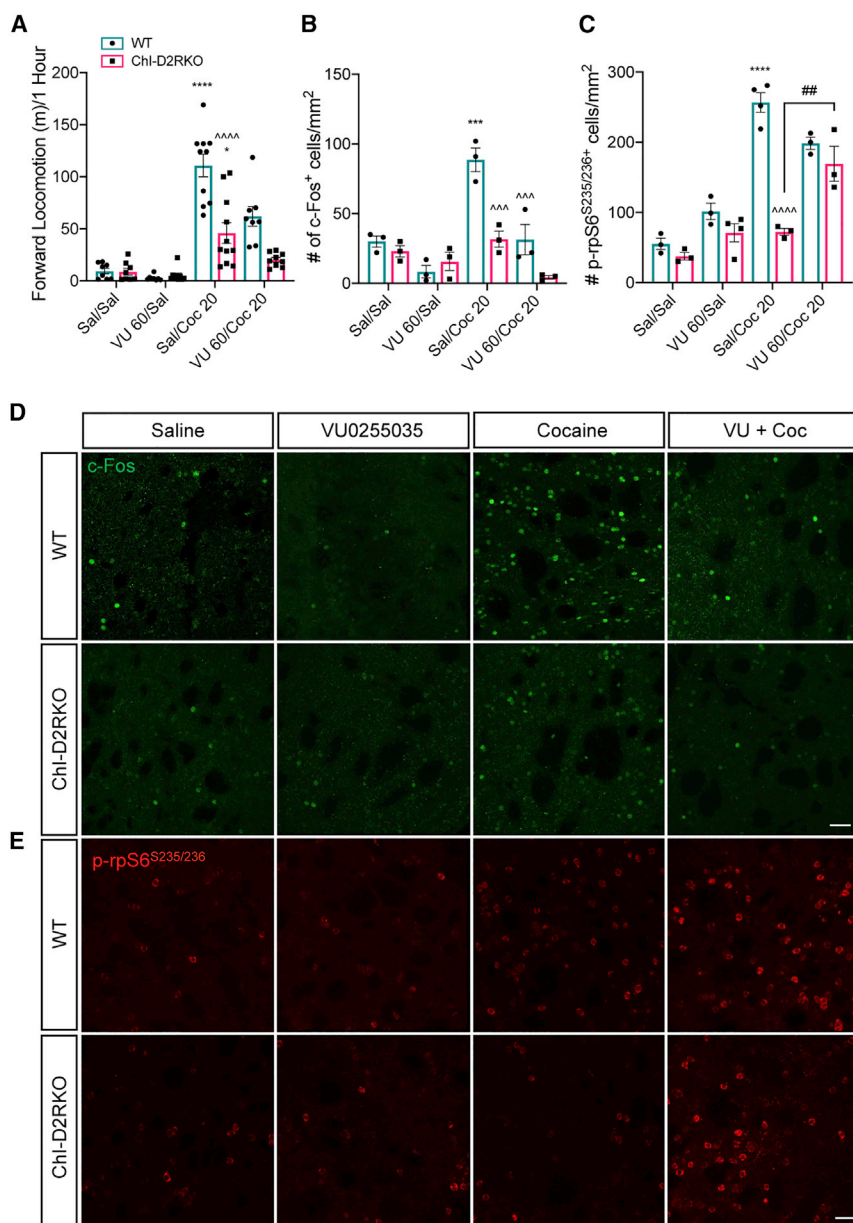
Figure 6. Antagonism of Muscarinic Receptors Enables Cocaine Response in ChI-D2RKO Mice

(A) The selective M1R antagonist fails to rescue cocaine-induced motor activity in ChI-D2RKO mice (n = 8–11/group). Genotype: $F_{(1, 63)}$ = 26.35, p < 0.0001; treatment: $F_{(3, 63)}$ = 49.22, p < 0.0001; interaction: $F_{(3, 63)}$ = 10.88, p < 0.0001.

(B and C) Quantification of the number of (B) c-Fos$^+$ neurons (2-way ANOVA; genotype: $F_{(1, 16)}$ = 21.85, p = 0.0003; treatment: $F_{(3, 16)}$ = 23.16, p < 0.0001; interaction: $F_{(3, 16)}$ = 9.701, p = 0.0007) and (C) p-rpS6$^{S235/236+}$ neurons per square millimeter within the DMS 1 h after cocaine (n = 3–6/group) (genotype: $F_{(1, 18)}$ = 49.10, p < 0.0001; treatment: $F_{(3, 18)}$ = 46.67, p < 0.0001; interaction: $F_{(3, 18)}$ = 18.86, p < 0.0001).

Bonferroni test: ***p < 0.001, ****p < 0.0001 versus saline of same genotype; ^^^p < 0.001, ^^^^p < 0.0001 versus WT Sal/Coc 20; #p < 0.05, ##p < 0.01, ####p < 0.0001 versus specified treatment with same genotype.

(D and E) Representative images of (D) c-Fos$^+$ neurons and (E) p-rpS6$^{S235/236+}$ neurons in the DMS of mice treated as in (A)–(C). Scale bar: 50 μm.

Values shown in (A)–(C) are mean ± SEM.

analyzing the ability to associate an environment with cocaine. For this, we performed the conditioned place preference (CPP) test on male mice of both genotypes. On day 1, a pre-conditioning test was performed, and the time spent by each mouse in the 2 compartments of the CPP apparatus was evaluated for 20 min. A drug-paired compartment was then randomly assigned to mice and conditioning started. Four groups of mice for each genotype were made: saline-saline, saline-cocaine (10 mg/kg, i.p.), saline-tropicamide (10 mg/kg, i.p.), and tropicamide-cocaine (10 mg/kg, i.p. of each drug). Tropicamide was administered 15 min before cocaine. During conditioning, mice were restricted for 20 min to either the drug-associated compartment where they received the drugs on days 2, 4, 6, and 8 or the other compartment where they received saline on days 3, 5, 7, and 9. On day 10, the preference for the drug-associated compartment was tested by leaving the mouse free to choose between compartments for 20 min (Figure 7A). Motor activity did not differ between genotypes either during the pre-conditioning (p = 0.3463) (Figure S5A) or during the test (p = 0.0555) (Figure S5B).

ChI-D2RKO mice did not demonstrate a significant CPP to cocaine as compared to WT mice (p = 0.0003) (Figure 7B), indicating that the reinforcing properties of cocaine are affected in ChI-D2RKO mice as compared to WT littermates. M4R antagonism before cocaine administration restored both cocaine-induced locomotion and CPP in ChI-D2RKO mice as compared to the cocaine-only group of the same genotype (p = 0.0223) and to WT levels (p > 0.99) (Figures 7B, S5C, and S5D).

Analyses of c-fos induction by FISH in striatal sections from mice sacrificed 1 h after the test session showed a blunted response both in the DMS (Figure S5E) and ventral striatum (Figure S5F) (DMS: p = 0.0145; ventral striatum: p = 0.0011) of ChI-D2RKO mice conditioned with cocaine as compared to WT controls. Analogous with the CPP results, prior tropicamide treatment during the conditioning phase rescued the c-fos deficit as compared to the cocaine-alone group of ChI-D2RKO mice (DMS: p = 0.0183; ventral striatum: p = 0.0254).

To assess whether the inhibitory D2R-mediated control of ChIs is required for the expression of reward, we analyzed
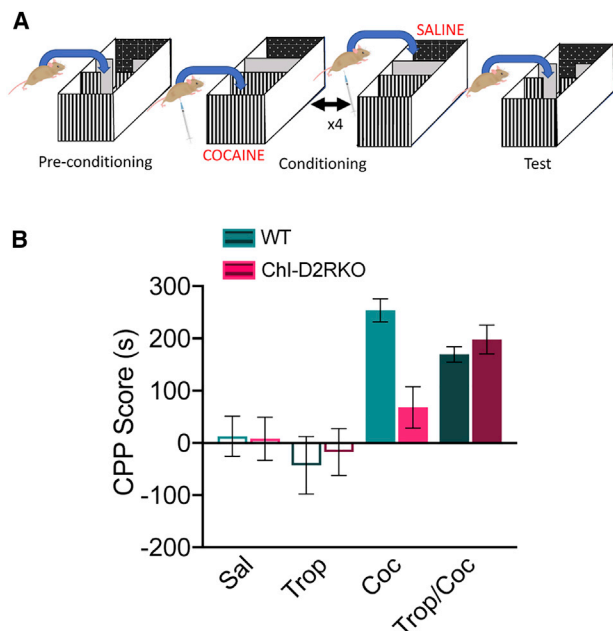
A

B

Figure 7. The Reinforcing Properties of Cocaine Are Affected by the Loss of Dopaminergic Inhibition of ChIs

(A) Illustration of the protocol used to perform the CPP test.

(B) CPP score after conditioning with either saline (Sal), tropicamide (Trop), cocaine (Coc), or Trop + Coc (Trop/Coc) in WT and ChI-D2RKO mice (n = 8–16/group). Genotype: $F_{(1, 76)}$ = 1.989, p = 0.1226; treatment: $F_{(3, 76)}$ = 12.84, p < 0.0001; interaction $F_{(3, 76)}$ = 3.756, p = 0.0143.

CPP in response to food (Cocoa Pebbles, Post Consumer Brands) as the reinforcer. The same CPP protocol was used, with the exception that Cocoa Pebbles replaced the drug in the compartment on days 2, 4, 6, and 8, and no food was presented in the opposite compartment on days 3, 5, 7, and 9. While WT mice displayed a strong place preference to the food-associated compartment (p = 0.0094), ChI-D2RKO mice did not (p > 0.99) (Figure S6A), despite normal consumption of Cocoa Pebbles during the conditioning phase. In agreement with this response, *c-fos* was induced in the DMS and the ventral striatum of WT mice (DMS: p = 0.0006; ventral striatum: p = 0.0002) but not of ChI-D2RKO mice, as evaluated 1 h after the test session (DMS: p = 0.6197; ventral striatum: p > 0.99) (Figures S6B and S6C).

The absence of CPP to cocaine and food in ChI-D2RKO mice appears independent from altered memory, as established by the absence of significant differences between male WT and ChI-D2RKO mice in the novel object recognition test (Figure S7). WT and ChI-D2RKO mice are equally able to recognize a novel object (Figures S7A and S7B) (p = 0.4178), with no differences in motor activity in the testing apparatus (Figure S7C) (p = 0.7129).

DISCUSSION

All drugs of abuse, including cocaine, increase DA signaling in the mesolimbic pathway, which is involved in the control of mo-

tor- and reward-related behaviors. The psychomotor effects of cocaine are mostly attributed to DA activation of dMSNs, resulting in the stimulation of the basal ganglia direct pathway (Bertran-Gonzalez et al., 2008; Zhang et al., 2002). Nevertheless, the DA-mediated effects of cocaine on dMSNs are regulated by iMSNs through D2Rs (Taverna et al., 2008; Kharkwal et al., 2016b; Lemos et al., 2016). In addition, striatal interneurons connecting to output MSNs (Cai and Ford, 2018; Francis et al., 2019; Gong and Ford, 2019; Mamaligas and Ford, 2016) and corticostriatal, thalamic, and mesolimbic afferents to MSNs and interneurons (Cai and Ford, 2018; Kosillo et al., 2016; Pancani et al., 2015; Qi et al., 2016) further enhance the level of complexity in unraveling how cocaine induces motor and reinforcing effects. In most of these connections, DA plays a critical role through activation of D2Rs. These receptors are located pre- and postsynaptically in striatal and afferent neurons. Thus, the role discovered for D2R in iMSNs in facilitating cocaine-mediated dMSNs responses (Kharkwal et al., 2016b; Lemos et al., 2016) may be a general feature of D2R signaling in the striatum. D2R activation may serve as a general modulator of the responses of dMSNs through heterologous control of striatal neurotransmitters and neuromodulators in neurons and afferents.

Our findings show that D2R activation is indeed central to ChIs. We show that the D2R-mediated inhibition of ChIs is required to maintain balanced cholinergic signals, which directly affect dMSN responses to cocaine. The loss of the D2R inhibitory control of ChIs results in significantly diminished motor and cellular responses to the drug. We hypothesized that this phenotype is the result of an increased cholinergic tone in striatal circuits due to the unopposed stimulation of D5Rs on ChIs and the consequent increase in ACh release. Our hypothesis is supported by the impaired response to cocaine of WT mice in which ACh degradation is inhibited using donepezil before cocaine administration (Figure 3A). In line with these findings, pharmacological approaches restored the acute effects of cocaine on motor and cellular responses in ChI-D2RKO mice; scopolamine administered before cocaine restored the cocaine-mediated motor and cellular effects to WT levels. We determined that the M4R-specific antagonist tropicamide (Figure 5), but not the M1R specific antagonist VU0255035 (Figure 6) gave the same effects as scopolamine (Figure 4). These results point to the important regulation of the activity of dMSNs by ACh through M4R signaling (Klawonn et al., 2018; Weiner et al., 1990). The observation that tropicamide reverses the phenotype of ChI-D2RKO excludes a possible interference of M4R autoreceptor blockade in these effects, which should further increase ACh release. In contrast, the presence of M4R on corticostriatal and thalamic fibers may greatly influence the activity of both dMSNs and iMSNs through modulating glutamate release (Yohn et al., 2018; Moehle and Conn, 2019). Our results showing the rescue of c-Fos induction by tropicamide suggests that cortical and thalamic fibers may well be affected by the increased ACh tone in ChI-D2RKO mice.

Silencing of ChIs through the expression of hM4Di in these neurons in the presence of CNO (Figure 3B) further supports our hypothesis of increased ACh signaling in ChI-D2RKO mice, since this manipulation restored the cocaine responses of mutant mice to WT levels. These results convincingly establish

that the basis of the altered cocaine effects in ChI-D2RKO mice is the increased ACh levels resulting from the absence of D2R signaling in ChIs.

The impaired behavioral response of ChI-D2RKO mice to the drug was paralleled by the absence of the induction of the immediate early gene c-*fos*. Induction of c-*fos*, a transcription factor of the AP1 family, is a hallmark of the cellular effect of drugs of abuse. This striking effect prompted us to perform a genome-wide analysis using RNA-seq comparing WT and ChI-D2RKO DMS transcriptomic profiles in the absence or presence of cocaine. These analyses revealed a reprogramming of gene expression profiles in the mutants as compared to equally treated WT mice in both conditions. Among the genes that were differentially expressed, c-*fos* was found to be among the most significant, thus validating our IF analyses. In addition to c-*fos*, other members of the AP1 family, together with other families of transcription factors, were found to be differentially expressed. The implication of the AP1 family *Egr*s and other transcription factors in the effects of cocaine emphasizes the immediate effect of cocaine in reprogramming genomic profiles, even after the first encounter with the drug, which likely leads to subsequent maladaptive changes in synaptic plasticity. In addition, our findings reveal that the D2R-mediated control of ACh signaling is critically linked to the effects of cocaine.

To explore the impact of altered cholinergic signaling in the more advanced stages of drug use, we used two behavioral paradigms: sensitization and CPP. Behavioral sensitization is related to changes in the motor effects of the drug while CPP correlates to the reward-related effects (Cunningham et al., 2006; Robinson and Berridge, 2008). Notably, ChI-D2RKO mice behaved differently from their WT littermates in both tests. We observed a partially escalating motor response to cocaine in ChI-D2RKO mice during the repetitive 5 days of treatment as compared to WT mice. However, after 1 week of withdrawal, a challenge injection to a lower dose of cocaine did not result in the expected enhanced response to the drug in the ChI-D2RKO as it did in WT mice. These results suggest that the D2R-mediated control of ACh signaling is required for the induction of long-term modifications leading to sensitization. We speculate that the absence or lowered inductions of the different transcription factors identified by RNA-seq could at least in part be responsible for the aberrant response. Similarly, unlike with WT, ChI-D2RKO mice appear insensitive to the reinforcing effects of cocaine and of food as measured by CPP. This result is highly relevant since the activity of ChIs contributes to associative learning (Brown et al., 2012; Zhang et al., 2018). ChIs receive dopaminergic, GABAergic, and glutamatergic signals from the ventral tegmental area (VTA) that induce the pausing of these neurons (Brown et al., 2012; Kharkwal et al., 2016a; Cai and Ford, 2018; Zhang and Cragg, 2017). The absence of D2Rs by removing the dopaminergic inhibitory input (Kharkwal et al., 2016a) may disrupt the ChI-dependent mechanism required to signal the saliency of an event or conversely signal any event as salient, making it difficult for the subject to associate the drug with the right compartment. These conclusions are supported by the effect of chemogenetic and pharmacological approaches in restoring sensitization and CPP.

In conclusion, the analysis of D2R cell-specific KO mice has been instrumental in clarifying the role of this receptor in the control of striatal circuits (Anzalone et al., 2012; Kharkwal et al., 2016b, 2016a; Lemos et al., 2016). The absence of D2R either in iMSN- or in ChI-D2RKO mice shows that D2R signaling in both neurons is a requirement for the control of dMSNs-mediated functions and cocaine-mediated effects. Our findings suggest that the identification of molecules downstream of D2R may offer leads in the treatment of cocaine addiction.

STAR★METHODS

Detailed methods are provided in the online version of this paper and include the following:

- KEY RESOURCES TABLE
- LEAD CONTACT AND MATERIALS AVAILABILITY
- EXPERIMENTAL MODEL AND SUBJECT DETAILS
- METHOD DETAILS
  - Stereotaxic Surgery
  - Drugs
  - Behavioral Analyses
  - RNA preparation for RNA-sequencing
  - Library Preparation for RNA-Sequencing
  - Bioinformatics
  - Immunofluorescence
  - Fluorescent *in situ* hybridization
- QUANTIFICATION AND STATISTICAL ANALYSIS
- DATA AND CODE AVAILABILITY

REFERENCES

Anzalone, A., Lizardi-Ortiz, J.E., Ramos, M., De Mei, C., Hopf, F.W., Iaccarino, C., Halbout, B., Jacobsen, J., Kinoshita, C., Welter, M., et al. (2012). Dual control of dopamine synthesis and release by presynaptic and postsynaptic dopamine D2 receptors. J. Neurosci. 32, 9023–9034.

Aosaki, T., Miura, M., Suzuki, T., Nishimura, K., and Masuda, M. (2010). Acetylcholine-dopamine balance hypothesis in the striatum: an update. Geriatr. Gerontol. Int. 10 (Suppl 1), S148–S157.

Berlanga, M.L., Simpson, T.K., and Alcantara, A.A. (2005). Dopamine D5 receptor localization on cholinergic neurons of the rat forebrain and diencephalon: a potential neuroanatomical substrate involved in mediating dopaminergic influences on acetylcholine release. J. Comp. Neurol. 492, 34–49.

Bertran-Gonzalez, J., Bosch, C., Maroteaux, M., Matamales, M., Hervé, D., Valjent, E., and Girault, J.-A. (2008). Opposing patterns of signaling activation in dopamine D1 and D2 receptor-expressing striatal neurons in response to cocaine and haloperidol. J. Neurosci. 28, 5671–5685.

Biever, A., Puighermanal, E., Nishi, A., David, A., Panciatici, C., Longueville, S., Xirodimas, D., Gangarossa, G., Meyuhas, O., Hervé, D., et al. (2015). PKA-dependent phosphorylation of ribosomal protein S6 does not correlate with translation efficiency in striatonigral and striatopallidal medium-sized spiny neurons. J. Neurosci. 35, 4113–4130.

Blighe, K., Rana, S., and Lewis, M. (2019). EnhancedVolcano: publication-ready volcano plots with enhanced colouring and labeling. Bioconductor version 3.10. https://bioconductor.org/packages/release/bioc/html/EnhancedVolcano.html.

Bonaventura, J., Eldridge, M.A., Hu, F., Gomez, J.L., Sanchez-Soto, M., Abramyan, A.M., Lam, S., Boehm, M., Ruiz, C., Farrell, M., et al. (2018). Chemogenetic ligands for translational neurotheranostics. Nat. Commun 10, 4627.

Boudreau, A.C., and Wolf, M.E. (2005). Behavioral sensitization to cocaine is associated with increased AMPA receptor surface expression in the nucleus accumbens. J. Neurosci. 25, 9144–9151.

Brown, M.T.C., Tan, K.R., O'Connor, E.C., Nikonenko, I., Muller, D., and Lüscher, C. (2012). Ventral tegmental area GABA projections pause accumbal cholinergic interneurons to enhance associative learning. Nature 492, 452–456.

Cai, Y., and Ford, C.P. (2018). Dopamine Cells Differentially Regulate Striatal Cholinergic Transmission across Regions through Corelease of Dopamine and Glutamate. Cell Rep. 25, 3148–3157.e3.

Carelli, R.M. (2002). Nucleus accumbens cell firing during goal-directed behaviors for cocaine vs. 'natural' reinforcement. Physiol. Behav. 76, 379–387.

Carlson, M., Pagès, H., Aboyoun, P., Falcon, S., Morgan, M., Sarkar, D., Lawrence, M., and Obenchain, V. (2019). GenomicFeatures: conveniently import and query gene models. Bioconductor version 3.10. https://bioconductor.org/packages/release/bioc/html/GenomicFeatures.html.

Centonze, D., Grande, C., Usiello, A., Gubellini, P., Erbs, E., Martin, A.B., Pisani, A., Tognazzi, N., Bernardi, G., Moratalla, R., et al. (2003). Receptor subtypes involved in the presynaptic and postsynaptic actions of dopamine on striatal interneurons. J. Neurosci. 23, 6245–6254.

Centonze, D., Gubellini, P., Usiello, A., Rossi, S., Tscherter, A., Bracci, E., Erbs, E., Tognazzi, N., Bernardi, G., Pisani, A., et al. (2004). Differential contribution of dopamine D2S and D2L receptors in the modulation of glutamate and GABA transmission in the striatum. Neuroscience 129, 157–166.

Chandra, R., and Lobo, M.K. (2017). Beyond Neuronal Activity Markers: Select Immediate Early Genes in Striatal Neuron Subtypes Functionally Mediate Psychostimulant Addiction. Front. Behav. Neurosci. 11, 112.

Cone, E.J. (1995). Pharmacokinetics and pharmacodynamics of cocaine. J. Anal. Toxicol. 19, 459–478.

Cunningham, C.L., Gremel, C.M., and Groblewski, P.A. (2006). Drug-induced conditioned place preference and aversion in mice. Nat. Protoc. 1, 1662–1670.

Curran, T., and Franza, B.R., Jr. (1988). Fos and Jun: the AP-1 connection. Cell 55, 395–397.

Day, J.J., Roitman, M.F., Wightman, R.M., and Carelli, R.M. (2007). Associative learning mediates dynamic shifts in dopamine signaling in the nucleus accumbens. Nat. Neurosci. 10, 1020–1028.

DeBoer, P., and Abercrombie, E.D. (1996). Physiological release of striatal acetylcholine in vivo: modulation by D1 and D2 dopamine receptor subtypes. J. Pharmacol. Exp. Ther. 277, 775–783.

Dobin, A., Davis, C.A., Schlesinger, F., Drenkow, J., Zaleski, C., Jha, S., Batut, P., Chaisson, M., and Gingeras, T.R. (2013). STAR: ultrafast universal RNA-seq aligner. Bioinformatics 29, 15–21.

Duclot, F., and Kabbaj, M. (2017). The Role of Early Growth Response 1 (EGR1) in Brain Plasticity and Neuropsychiatric Disorders. Front. Behav. Neurosci. 11, 35.

Fosnaugh, J.S., Bhat, R.V., Yamagata, K., Worley, P.F., and Baraban, J.M. (1995). Activation of arc, a putative "effector" immediate early gene, by cocaine in rat brain. J. Neurochem. 64, 2377–2380.

Francis, T.C., Yano, H., Demarest, T.G., Shen, H., and Bonci, A. (2019). High-Frequency Activation of Nucleus Accumbens D1-MSNs Drives Excitatory Potentiation on D2-MSNs. Neuron 103, 432–444.e3.

Gao, P., Limpens, J.H.W., Spijker, S., Vanderschuren, L.J.M.J., and Voorn, P. (2017). Stable immediate early gene expression patterns in medial prefrontal cortex and striatum after long-term cocaine self-administration. Addict. Biol. 22, 354–368.

Gong, S., and Ford, C.P. (2019). Cholinergic Interneurons Provide a Link to Balance Excitation across Striatal Output Neurons. Neuron 103, 351–353.

Gonzales, B.J., Mukherjee, D., Ashwal-Fluss, R., Loewenstein, Y., and Citri, A. (2019). Subregion-specific rules govern the distribution of neuronal immediate-early gene induction. Proc. Natl. Acad. Sci. USA, Published online October 21, 2019. https://doi.org/10.1073/pnas.1913658116.

Graveland, G.A., and DiFiglia, M. (1985). The frequency and distribution of medium-sized neurons with indented nuclei in the primate and rodent neostriatum. Brain Res. 327, 307–311.

Graybiel, A.M., Aosaki, T., Flaherty, A.W., and Kimura, M. (1994). The basal ganglia and adaptive motor control. Science 265, 1826–1831.

Hope, B., Kosofsky, B., Hyman, S.E., and Nestler, E.J. (1992). Regulation of immediate early gene expression and AP-1 binding in the rat nucleus accumbens by chronic cocaine. Proc. Natl. Acad. Sci. USA 89, 5764–5768.

Hope, B.T., Simmons, D.E., Mitchell, T.B., Kreuter, J.D., and Mattson, B.J. (2006). Cocaine-induced locomotor activity and Fos expression in nucleus accumbens are sensitized for 6 months after repeated cocaine administration outside the home cage. Eur. J. Neurosci. 24, 867–875.

Hyman, S.E., and Malenka, R.C. (2001). Addiction and the brain: the neurobiology of compulsion and its persistence. Nat. Rev. Neurosci. 2, 695–703.

Hyman, S.E., Malenka, R.C., and Nestler, E.J. (2006). Neural mechanisms of addiction: the role of reward-related learning and memory. Annu. Rev. Neurosci. 29, 565–598.

Jenab, S., Festa, E.D., Russo, S.J., Wu, H.B.K., Inturrisi, C.E., and Quinones-Jenab, V. (2003). MK-801 attenuates cocaine induction of c-fos and preprodynorphin mRNA levels in Fischer rats. Brain Res. Mol. Brain Res. 117, 237–239.

Jeon, J., Dencker, D., Wörtwein, G., Woldbye, D.P.D., Cui, Y., Davis, A.A., Levey, A.I., Schütz, G., Sager, T.N., Mørk, A., et al. (2010). A subpopulation of neuronal M4 muscarinic acetylcholine receptors plays a critical role in modulating dopamine-dependent behaviors. J. Neurosci. 30, 2396–2405.

Kalivas, P.W., and Stewart, J. (1991). Dopamine transmission in the initiation and expression of drug- and stress-induced sensitization of motor activity. Brain Res. Brain Res. Rev. 16, 223–244.

Karvat, G., and Kimchi, T. (2014). Acetylcholine elevation relieves cognitive rigidity and social deficiency in a mouse model of autism. Neuropsychopharmacology 39, 831–840.

Keenan, A.B., Torre, D., Lachmann, A., Leong, A.K., Wojciechowicz, M.L., Utti, V., Jagodnik, K.M., Kropiwnicki, E., Wang, Z., and Ma'ayan, A. (2019). ChEA3: transcription factor enrichment analysis by orthogonal omics integration. Nucleic Acids Res. 47 (W1), W212–W224.

Kharkwal, G., Brami-Cherrier, K., Lizardi-Ortiz, J.E., Nelson, A.B., Ramos, M., Del Barrio, D., Sulzer, D., Kreitzer, A.C., and Borrelli, E. (2016a). Parkinsonism Driven by Antipsychotics Originates from Dopaminergic Control of Striatal Cholinergic Interneurons. Neuron *91*, 67–78.

Kharkwal, G., Radl, D., Lewis, R., and Borrelli, E. (2016b). Dopamine D2 receptors in striatal output neurons enable the psychomotor effects of cocaine. Proc. Natl. Acad. Sci. USA *113*, 11609–11614.

Klawonn, A.M., Wilhelms, D.B., Lindström, S.H., Singh, A.K., Jaarola, M., Wess, J., Fritz, M., and Engblom, D. (2018). Muscarinic M4 Receptors on Cholinergic and Dopamine D1 Receptor-Expressing Neurons Have Opposing Functionality for Positive Reinforcement and Influence Impulsivity. Front. Mol. Neurosci. *11*, 139.

Kosillo, P., Zhang, Y.-F., Threlfell, S., and Cragg, S.J. (2016). Cortical Control of Striatal Dopamine Transmission via Striatal Cholinergic Interneurons. Cereb. Cortex *26*, 4160–4169.

Lawrence, M., Huber, W., Pagès, H., Aboyoun, P., Carlson, M., Gentleman, R., Morgan, M.T., and Carey, V.J. (2013). Software for computing and annotating genomic ranges. PLoS Comput. Biol. *9*, e1003118.

Lemos, J.C., Friend, D.M., Kaplan, A.R., Shin, J.H., Rubinstein, M., Kravitz, A.V., and Alvarez, V.A. (2016). Enhanced GABA Transmission Drives Bradykinesia Following Loss of Dopamine D2 Receptor Signaling. Neuron *90*, 824–838.

Lim, S.A.O., Kang, U.J., and McGehee, D.S. (2014). Striatal cholinergic interneuron regulation and circuit effects. Front. Synaptic Neurosci. *6*, 22.

Lobo, M.K., and Nestler, E.J. (2011). The striatal balancing act in drug addiction: distinct roles of direct and indirect pathway medium spiny neurons. Front. Neuroanat. *5*, 41.

Love, M., Ahlmann-Eltze, C., Anders, S., and Huber, W. (2019). DESeq2: differential gene expression analysis based on the negative binomial distribution. Bioconductor version 3.10. https://bioconductor.org/packages/release/bioc/html/DESeq2.html.

Mamaligas, A.A., and Ford, C.P. (2016). Spontaneous Synaptic Activation of Muscarinic Receptors by Striatal Cholinergic Neuron Firing. Neuron *91*, 574–586.

Marche, K., Martel, A.-C., and Apicella, P. (2017). Differences between Dorsal and Ventral Striatum in the Sensitivity of Tonically Active Neurons to Rewarding Events. Front. Syst. Neurosci. *11*, 52.

McClung, C.A., and Nestler, E.J. (2003). Regulation of gene expression and cocaine reward by CREB and DeltaFosB. Nat. Neurosci. *6*, 1208–1215.

Moehle, M.S., and Conn, P.J. (2019). Roles of the M4 acethylcholine receptor in the basal ganglia and the treatment of movement disorders. Mov. Disord. *34*, 1089–1099.

Moehle, M.S., Pancani, T., Byun, N., Yohn, S.E., Wilson, G.H., 3rd, Dickerson, J.W., Remke, D.H., Xiang, Z., Niswender, C.M., Wess, J., et al. (2017). Cholinergic Projections to the Substantia Nigra Pars Reticulata Inhibit Dopamine Modulation of Basal Ganglia through the M₄ Muscarinic Receptor. Neuron *96*, 1358–1372.e4.

Nelson, A.B., and Kreitzer, A.C. (2014). Reassessing models of basal ganglia function and dysfunction. Annu. Rev. Neurosci. *37*, 117–135.

Oldenburg, I.A., and Ding, J.B. (2011). Cholinergic modulation of synaptic integration and dendritic excitability in the striatum. Curr. Opin. Neurobiol. *21*, 425–432.

Oorschot, D.E. (2013). The percentage of interneurons in the dorsal striatum of the rat, cat, monkey and human: a critique of the evidence. Basal Ganglia *3*, 19–24.

Pagès, H., Obenchain, V., and Morgan, M. (2019). GenomicAlignments: Representation and manipulation of short genomic alignments. Bioconductor version 3.10. https://bioconductor.org/packages/release/bioc/html/GenomicAlignments.html.

Pancani, T., Foster, D.J., Moehle, M.S., Bichell, T.J., Bradley, E., Bridges, T.M., Klar, R., Poslusney, M., Rook, J.M., Daniels, J.S., et al. (2015). Allosteric activation of M4 muscarinic receptors improve behavioral and physiological alterations in early symptomatic YAC128 mice. Proc. Natl. Acad. Sci. USA *112*, 14078–14083.

Philibin, S.D., Hernandez, A., Self, D.W., and Bibb, J.A. (2011). Striatal signal transduction and drug addiction. Front. Neuroanat. *5*, 60.

Pisani, A., Bonsi, P., Centonze, D., Calabresi, P., and Bernardi, G. (2000). Activation of D2-like dopamine receptors reduces synaptic inputs to striatal cholinergic interneurons. J. Neurosci. *20*, RC69.

Puighermanal, E., Biever, A., Pascoli, V., Melser, S., Pratlong, M., Cutando, L., Rialle, S., Severac, D., Boubaker-Vitre, J., Meyuhas, O., et al. (2017). Ribosomal Protein S6 Phosphorylation Is Involved in Novelty-Induced Locomotion, Synaptic Plasticity and mRNA Translation. Front. Mol. Neurosci. *10*, 419.

Qi, J., Zhang, S., Wang, H.-L., Barker, D.J., Miranda-Barrientos, J., and Morales, M. (2016). VTA glutamatergic inputs to nucleus accumbens drive aversion by acting on GABAergic interneurons. Nat. Neurosci. *19*, 725–733.

Robinson, T.E., and Berridge, K.C. (2008). Review. The incentive sensitization theory of addiction: some current issues. Philos. Trans. R. Soc. Lond. B Biol. Sci. *363*, 3137–3146.

Roth, B.L. (2016). DREADDs for Neuroscientists. Neuron *89*, 683–694.

Sheffler, D.J., Williams, R., Bridges, T.M., Xiang, Z., Kane, A.S., Byun, N.E., Jadhav, S., Mock, M.M., Zheng, F., Lewis, L.M., et al. (2009). A novel selective muscarinic acetylcholine receptor subtype 1 antagonist reduces seizures without impairing hippocampus-dependent learning. Mol. Pharmacol. *76*, 356–368.

Shen, W., Tian, X., Day, M., Ulrich, S., Tkatch, T., Nathanson, N.M., and Surmeier, D.J. (2007). Cholinergic modulation of Kir2 channels selectively elevates dendritic excitability in striatopallidal neurons. Nat. Neurosci. *10*, 1458–1466.

Su, Y., Shin, J., Zhong, C., Wang, S., Roychowdhury, P., Lim, J., Kim, D., Ming, G.-L., and Song, H. (2017). Neuronal activity modifies the chromatin accessibility landscape in the adult brain. Nat. Neurosci. *20*, 476–483.

Surmeier, D.J., Plotkin, J., and Shen, W. (2009). Dopamine and synaptic plasticity in dorsal striatal circuits controlling action selection. Curr. Opin. Neurobiol. *19*, 621–628.

Taverna, S., Ilijic, E., and Surmeier, D.J. (2008). Recurrent collateral connections of striatal medium spiny neurons are disrupted in models of Parkinson's disease. J. Neurosci. *28*, 5504–5512.

Thiriet, N., Aunis, D., and Zwiller, J. (2000). C-fos and egr-1 immediate-early gene induction by cocaine and cocaethylene in rat brain: a comparative study. Ann. N Y Acad. Sci. *914*, 46–57.

Threlfell, S., Clements, M.A., Khodai, T., Pienaar, I.S., Exley, R., Wess, J., and Cragg, S.J. (2010). Striatal muscarinic receptors promote activity dependence of dopamine transmission via distinct receptor subtypes on cholinergic interneurons in ventral versus dorsal striatum. J. Neurosci. *30*, 3398–3408.

Torres, G., and Rivier, C. (1993). Cocaine-induced expression of striatal c-fos in the rat is inhibited by NMDA receptor antagonists. Brain Res. Bull. *30*, 173–176.

Valjent, E., Corvol, J.-C., Pagès, C., Besson, M.-J., Maldonado, R., and Caboche, J. (2000). Involvement of the extracellular signal-regulated kinase cascade for cocaine-rewarding properties. J. Neurosci. *20*, 8701–8709.

Volakakis, N., Kadkhodaei, B., Joodmardi, E., Wallis, K., Panman, L., Silvaggi, J., Spiegelman, B.M., and Perlmann, T. (2010). NR4A orphan nuclear receptors as mediators of CREB-dependent neuroprotection. Proc. Natl. Acad. Sci. USA *107*, 12317–12322.

Weiner, D.M., Levey, A.I., and Brann, M.R. (1990). Expression of muscarinic acetylcholine and dopamine receptor mRNAs in rat basal ganglia. Proc. Natl. Acad. Sci. USA *87*, 7050–7054.

Xu, M., Moratalla, R., Gold, L.H., Hiroi, N., Koob, G.F., Graybiel, A.M., and Tonegawa, S. (1994). Dopamine D1 receptor mutant mice are deficient in striatal expression of dynorphin and in dopamine-mediated behavioral responses. Cell *79*, 729–742.

Yohn, S.E., Foster, D.J., Covey, D.P., Moehle, M.S., Galbraith, J., Garcia-Barrantes, P.M., Cho, H.P., Bubser, M., Blobaum, A.L., Joffe, M.E., et al. (2018). Activation of the mGlu₁ metabotropic glutamate receptor has antipsychotic-like effects and is required for efficacy of M₄ muscarinic receptor allosteric modulators. Mol. Psychiatry, Published online August 16, 2018. https://doi.org/10.1038/s41380-018-0206-2.

Young, S.T., Porrino, L.J., and Iadarola, M.J. (1991). Cocaine induces striatal c-fos-immunoreactive proteins via dopaminergic D1 receptors. Proc. Natl. Acad. Sci. USA *88*, 1291–1295.

Zhang, Y.-F., and Cragg, S.J. (2017). Pauses in Striatal Cholinergic Interneurons: What is Revealed by Their Common Themes and Variations? Front. Syst. Neurosci. *11*, 80.

Zhang, D., Zhang, L., Lou, D.W., Nakabeppu, Y., Zhang, J., and Xu, M. (2002). The dopamine D1 receptor is a critical mediator for cocaine-induced gene expression. J. Neurochem. *82*, 1453–1464.

Zhang, Y.-F., Reynolds, J.N.J., and Cragg, S.J. (2018). Pauses in Cholinergic Interneuron Activity Are Driven by Excitatory Input and Delayed Rectification, with Dopamine Modulation. Neuron *98*, 918–925.e3.

STAR★METHODS

KEY RESOURCES TABLE

REAGENT or RESOURCE	SOURCE	IDENTIFIER
Antibodies		
Rabbit anti-c-fos	Abcam	Cat# ab190289; RRID:AB_2737414
Rabbit anti-phospho-S6 Ribosomal Protein (Ser235/236)	Cell Signaling	Cat# 2211; RRID:AB_331679
Goat anti-choline acetyltransferase	Millipore/Sigma	Cat# AB144P; RRID:AB_2079751
Mouse anti-mCherry	Abcam	Cat# ab167453; RRID:AB_2571870
Sheep anti-digoxigenin-AP Fab fragments	Roche	Cat# 11093274910; RRID:AB_2734716
Sheep anti-fluorescein-POD Fab fragments	Roche	Cat# 11426346910; RRID:AB_840257
Donkey anti-goat Alexa Fluor 488	Abcam	Cat# ab150129; RRID:AB_2687506
Goat anti-rabbit Alexa Fluor 488	ThermoFisher	Cat# A-11034; RRID:AB_2576217
Goat anti-rabbit Alexa Fluor 546	ThermoFisher	Cat# A-11010; RRID:AB_2534077
Goat anti-mouse Alexa Fluor 546	ThermoFisher	Cat# A-11003; RRID:AB_141370
Bacterial and Virus Strains		
pAAV-hSyn-DIO-hM4D(Gi)-mCherry	AddGene	44362-AAV2
Critical Commercial Supplies		
DIG RNA Labeling Kit	Roche	11175025910
Fluorescein RNA Labeling Kit	Roche	11685619910
TSA Fluorescein Kit	Perkin Elmer	SAT701001KT
HNPP Fluorescent Detection Set	Roche	11758888001
Chemicals, Peptides, and Recombinant Proteins		
Cocaine HCl	Sigma	C5776
Donepezil HCl	Sigma	D6821
Scopolamine HBr Trihydrate	Sigma	PHR1470
Tropicamide HCl	Tocris	0909
VU0255035 HCl	UCI	N/A
Clozapine-N-Oxide	NIH	027862
JHU37160	HelloBio	HB6261
Deposited Data		
Raw and processed RNA-Seq Data	This Paper	ArrayExpress: E-MTAB-8589
Software and Algorithms		
Prism 8.3.0	GraphPad	https://www.graphpad.com/scientific-software/prism/
Viewpoint VideoTack	ViewPoint Behavior Technology	http://www.viewpoint.fr/en/p/software/videotrack
HCS 3.4.0.38	Illumina	https://support.illumina.com/downloads/hiseq-4000-3000-hcs-v3-4-0.html
Leica Application Suite X v 3.7.0	Leica	https://www.leica-microsystems.com/products/microscope-software/p/leica-las-x-ls/
FastQC	Babraham Bioinformatics	https://www.bioinformatics.babraham.ac.uk/projects/fastqc/
STAR 2.6.0c	Dobin et al., 2013	https://github.com/alexdobin/STAR/releases
Genomic Features	Lawrence et al., 2013	https://bioconductor.org/packages/release/bioc/html/GenomicFeatures.html
Genomic Alignments	Lawrence et al., 2013	https://bioconductor.org/packages/release/bioc/html/GenomicAlignments.html
DESeq2	Love et al., 2019	https://bioconductor.org/packages/release/bioc/html/DESeq2.html

(Continued on next page)

REAGENT or RESOURCE	SOURCE	IDENTIFIER
EnhancedVolcano	Blighe et al., 2019	https://bioconductor.org/packages/release/bioc/html/EnhancedVolcano.html
DAVID v6.8	The Database for Annotation, Visualization and Integrated Discovery	https://david.ncifcrf.gov/home.jsp
ChEA3	Keenan et al., 2019	https://amp.pharm.mssm.edu/chea3/

LEAD CONTACT AND MATERIALS AVAILABILITY

Further information and requests for resources and reactions should be directed to and fulfilled by the Lead Contact, Emiliana Borrelli (borrelli@uci.edu). All unique/stable materials and models generated from this study are available from the Lead Contact with a completed Materials Transfer Agreement.

EXPERIMENTAL MODEL AND SUBJECT DETAILS

All protocols were submitted and approved by the University of California, Irvine Institutional Animal Care and Use Committee in accordance with the National Institute of Health guidelines. Mice were group housed and maintained at standard 12h/12h light/dark cycle, at ~25°C, and humidity levels at 45%–60%. Animals were group housed and fed *ad libitum* unless otherwise specified. Female ChI-D2RKO and WT littermates mice did not differ in motor behavior compared to male mice in their response to cocaine and therefore all experiments were performed in males. Thus, we exclusively used adult male mice aged 8 to 14 weeks old for all experiments. ChI-D2RKO mice were generated by mating D2R^{floxflox} mice (used as WT controls) with choline acetyltransferase (ChAT)-Cre mice generating D2R$^{floxflox/ChAT\ Cre/+}$ mice, as previously described (Kharkwal et al., 2016a). For all behavioral testing, mice were manipulated at least 2 days prior to experimental start for 5 min/day.

METHOD DETAILS

Stereotaxic Surgery

3% vaporized isoflurane (Kent Scientific) was used to anesthetize mice before they were placed in the stereotaxic frame (David Kopf Instruments). A nose cone was placed over the mouse and isoflurane concentration was lowered to 1%–2%; temperature and breathing were closely monitored throughout the surgery. Adeno-associated viruses carrying designer receptors exclusively activated by designer drugs (DREADD) hM4Di (AAV-hSyn-DIO-hM4D(Gi)-mCherry; AddGene) were injected with in the dorsomedial striatum (DMS) (anterior-posterior, 0.98 mm; medial-lateral, ± 1.2 mm; dorso-ventral, −3 mm, from Bregma) according to the mouse brain atlas. 1.5 μL (6900 Genome Copies/hemisphere) were infused bilaterally over a period of 3 min. Following surgery, mice were monitored daily for at least 14 days prior to experiments.

Drugs

Cocaine HCl (Sigma), Tropicamide HCl (Tocris), Scopolamine HBr Trihydrate (Sigma), Donepezil HCl (Sigma), VU0255035 HCl (UCI), Clozapine-N-Oxide (CNO) (NIH), and JHU37160 dihydrochloride (J60) (HelloBio) were dissolved in sterile saline (0.9% NaCl pH 7.4). All drugs were administered intraperitoneally.

Behavioral Analyses

Acute

Locomotor activity was analyzed and recorded in a novel home cage (NHC) (20 cm × 30 cm x 13 cm transparent plastic box) using a video-tracking system (Viewpoint; Lyon France). Mice were habituated to the NHC for 2 hours prior to administration of saline or cocaine; motor behavior was monitored for the following hour. For experiments requiring the use of scopolamine, tropicamide, VU0255035, or donepezil, mice were habituated in their NHC for 2 hours, then administered these pharmacological agents or saline. 15 minutes later, mice were then given either saline or cocaine and motor responses recorded for the following hour. Experiments requiring the use of DREADD agonists were performed in the same way with the exception that cocaine or saline was given 30 minutes after CNO.

Sensitization

As in acute experiments, locomotor activity was analyzed and recorded in a NHC using video-tracking. Mice were habituated to their NHC for 30 minutes each day of the experiment; during the first two days of the protocol, all mice received only saline. The following 5 days, mice were given cocaine (15 mg/kg; ip) after 30 minutes of habituation and motor response was recorded for the following hour. After a one-week withdrawal period, mice were challenged with a lower dose of cocaine (10 mg/kg; ip) using the same method.

For experiments using the DREADD system, hM4Di ChI-D2RKO mice were injected with clozapine-N-oxide (3 mg/kg; ip) or J60 (0.1 mg/kg; ip) immediately before the 30-minute habituation period.

Cocaine Conditioned Place Preference

The CPP testing apparatus consisted of two compartments (15.5 cm x 16.5 cm x 20.3 cm) divided by a neutral space (15.5 cm x 5 cm x 20.3 cm); each compartment contained visual and tactile cues on the walls and floors. Each genotype was divided into two groups by conditioning mice to receive either saline or cocaine (10 mg/kg; ip) in a specific compartment. On day 1, mice were placed into the apparatus for 20 minutes and left free to explore both sides of the apparatus; time spent in each compartment was recorded and scored. The following day, conditioning started using an unbiased protocol in which the drug-paired compartment was randomly assigned to mice in each group. During conditioning, mice were given either cocaine or saline on alternate days and restricted to the appropriate compartment for 20 minutes. Cocaine was administered on days 2, 4, 6, and 8 with alternating saline injections on days 3, 5, 7, and 9. On day 10, the CPP test was performed by leaving the mice free of choosing between the two compartments for 20 minutes. Tropicamide (10 mg/kg; ip) was administered 15 minutes before saline or cocaine treatments on days 2, 4, 6, and 8.

Food Conditioned Place Preference

Food CPP was performed on mice that were food restricted to lose 10% of their starting body weight. After this, mice selected to be given the food reward were exposed to the reinforcer, Post Cocoa Pebbles cereal, for 2 days until all mice were observed eating the food reward. Then, CPP was performed using the same experimental timeline as the cocaine CPP. Five pieces of cereal were placed inside the food-paired room on days 2, 4, 6, and 8 with mice receiving nothing in the other compartment on days 3, 5, 7, and 9. For cocaine and food experiments, a CPP score was calculated by determining the difference between time spent in the reward associated compartment before and after conditioning.

Novel Object Recognition Test

Mice were habituated to the open-field testing apparatus (30 cm x 30 cm x 19 cm white box) 3 times for 5 minutes with 1 hour in between each habitation session. The following day, mice underwent a training session for 10 minutes during which each object was positioned 6 cm away from diagonal corners of the apparatus. On the testing day, 1 object was replaced with a novel object in a manner that was counter balanced, and mice were place in the apparatus for 10 minutes while being video tracked (See Figure S7A). Time investigating the object was determined as the time spent in a 4 cm x 4 cm area surrounding the object. The ability to discriminate between the known object and the novel object was calculated as a discrimination index using the formula $(time_{novel} - time_{known}) / (time_{novel} + time_{known})$.

RNA preparation for RNA-sequencing

After behavioral testing, brains were dissected and were rapidly frozen in 2-methylbutane on dry ice. For RNA preparation, bilateral tissue punches were obtained and rapidly homogenized in Trizol (Thermo Fisher) using a 26 ½ gauge needle attached to a 1 mL syringe. RNA isolation was completed following the manufacturer's protocol. RNA was resuspended in H_2O.

Library Preparation for RNA-Sequencing

Library preparation and sequencing were performed at the University of California, Irvine Genomic High-Throughput Facility. Total RNA was monitored for quality control using the Nanodrop absorbance ratios for 260/280nm and 260/230nm and the Agilent Bioanalyzer Nano RNA chip (Table S1). Library construction was performed according to the Illumina TruSeq® Stranded mRNA Sample Preparation Guide. The input quantity for total RNA was 150 ng and mRNA was enriched using oligo dT magnetic beads. The enriched mRNA was chemically fragmented for three minutes. First strand synthesis used random primers and reverse transcriptase to make cDNA. After second strand synthesis the double stranded cDNA was cleaned using AMPure XP beads and the cDNA was end repaired and then the 3′ ends were adenylated. Illumina barcoded adapters were ligated on the ends and the adaptor ligated fragments were enriched by nine cycles of PCR. The resulting libraries were validated by qPCR and sized by Agilent Bioanalyzer DNA high sensitivity chip. The concentrations for the libraries were normalized and then multiplexed together. The multiplexed libraries were sequenced on four lanes using single end 100 cycles chemistry on the HiSeq 4000. The version of HiSeq control software was HCS 3.4.0.38 with real time analysis software.

Bioinformatics

Read quality was assessed by FastQC (www.bioinformatics.babraham.ac.uk/projects/fastqc/). Sequence alignment was performed using the *Mus musculus* GENCODE reference genome (GTF file from release M23 GRCm38.p6) using STAR 2.6.0c software (Dobin et al., 2013) (Table S2). Annotation and count matrices were generated using Genomic Features (Carlson et al., 2019) and Genomic Alignments (Pagès et al., 2019). Differential expression analysis was performed using DESeq2 (Love et al., 2019). Read counts were normalized using the relative log expression method of DESeq2. Normalized read counts were converted into the log-read counts which were then used for identifying differentially expressed genes; in our comparisons saline treated WT mice were used as the control. Unadjusted and adjusted p values were determined for each gene; $p < 0.05$ was considered statistically significant. Volcano plots were generated using the EnhancedVolcano R package (Blighe et al., 2019). Biological processes represented by the differentially expressed genes were determined using the Database for Annotation, Visualization, and Integrated Discovery (DAVID) annotation tool (v. 6.8). Genes with a significance $p < 0.05$ and a Log2 Fold-Change greater than 1 and less than -1 were compiled and entered into DAVID; Benjamini test $p < 0.05$ was considered significant. Transcription factor enrichment analysis was performed using ChEA3

(Keenan et al., 2019). 969 differentially expressed genes from our differential expression analysis in cocaine treated mice were used. Data shown is from the "Top Rank" library option. The top 25 transcription factors obtained from this analysis were compared against the 60 most significant differentially expressed genes (padj < 0.05).

Immunofluorescence

1-hour after cocaine or saline administration, mice were deeply anesthetized with Euthasol followed by transcardial perfusion with 4% paraformaldehyde in PBS (Na_2HPO_4 10 mM, KH_2PO_4 1.8 mM, NaCl 137 mM, KCl 2.7 mM). Whole brains were then post-fixed over-night in 4% paraformaldehyde in PBS. 30 μm coronal striatal sections were obtained using a vibratome (Leica) and preserved in a cryoprotectant (30% glycerol and 30% ethylene glycol in PBS) and stored at −20C until use.

Tissue sections were washed three times in PBS, permeabilized for 15 min using 0.5% Triton X-100 in PBS and then rinsed twice in same buffer. Non-specific site were blocked by incubation in PBS with 5% Normal Goat Serum (NGS) for 1 hour at room temperature. Sections were incubated with primary antibodies: rabbit anti-c-*fos* (1:3000; Abcam), rabbit anti-p-rpS6$^{S235/236}$ (1:1000; Cell Signaling), goat anti-choline acetyltransferase (1:800; Millipore), and mouse anti-mCherry (1:800; Abcam) in PBS 1% NGS overnight at 4°C alone or in combination. The following day, sections were rinsed three times in PBS for 10 min. Sections were then incubated in secondary antibodies (goat anti-rabbit Alexa Fluor 488, donkey anti-goat Alexa Fluor 488, or goat anti-mouse Alexa Fluor 546) which were used at a 1:2000 concentration in PBS 1% NGS. The sections were rinsed twice with PBS before nuclei were stained with Draq 7 (1:1000; Biostatus). Images were taken on an SP5 confocal microscope (Leica). Striatal neurons positive for c-Fos or p-rpS6$^{S235/236}$ were quantified using LAS-X (Leica; version 3.7.0) software. Three 387.5 × 387.5 μm regions of interest in the dorsomedial and ventral striatum from 3-8 mice/treatment/genotype were used in experimenter blinded analyses. Values shown from IF experiments are represented as cell counts per mm^2.

Fluorescent *in situ* hybridization

Brain sections were obtained and hybridized with fluorescein-labeled *D1R or enkephalin (Enk)* and digoxigenin (DIG)-labeled *c-fos* riboprobes (Roche), as previously described (Anzalone et al., 2012; Kharkwal et al., 2016b), followed by anti–Fluorescein-POD (1:1000, Roche) and anti–DIG-AP (1:1000, Roche) antibodies. To amplify the signal the TSA PLUS fluorescein System (Perkin Elmer) and HNPP (2-hydroxy-3-naphtoic acid-2′-phenylanilide phosphate) fluorescent Detection Set (Roche) were used. Nuclei were stained with Draq7 1:1000. The percentage of double positive *c-fos* and *D1R or Enk* cells compared to the total *D1R or Enk* positive cells were determined. 3 mice/treatment/genotype were used in experimenter blinded analyses.

QUANTIFICATION AND STATISTICAL ANALYSIS

All values are presented as mean ± SEM. GraphPad Prism 8.3.0 (La Jolla California, USA) was used to perform statistical analyses. One, Two, or Three-way Analysis of Variance (ANOVA) followed by Bonferroni's multiple comparison post hoc test was used as appropriate; p < 0.05 was considered statistically significant.

DATA AND CODE AVAILABILITY

The accession number for the RNA-sequencing data set reported in this paper is ArrayExpress: E-MTAB-8589.